

# **FINAL REPORT**

**AWARD NUMBER: DE-FC36-99ID13819**

**Period: September 30, 1999 – August 12, 2005**

## **CONTROLLED THERMO-MECHANICAL PROCESSING OF TUBES AND PIPES FOR ENHANCED MANUFACTURING AND PERFORMANCE**

### **THE TIMKEN COMPANY – Prime Recipient**

Alloy Steel Business

Project Manager: Robert V. Kolarik II (330-471-2378)

1835 Dueber Avenue, S.W.

Mail Code: RES-04

P.O. Box 6930

Canton, Ohio 44706-0930

**November 11, 2005**

**Prepared for**

**U.S. DEPARTMENT OF ENERGY**

**Golden Field Office**

**1617 Cole Boulevard**

**Golden, Colorado 80401-3393**

**Project Team Members (as they existed at the time of the award)**

Colorado School of Mines  
Golden, Colorado 80401

CSM Project Leader:  
Mark T. Lusk (303-273-3675)

Ford Motor Company  
24500 Glendale Avenue  
Redford, Michigan 48239

Ford Project Leader:  
Claude M. Mack (313-592-2665)

Friedrich Kocks GmbH & Co.  
P.O. Box 100753  
40707 Hilden, Germany

Kocks Project Leader:  
Rötger Teyke (49-2103-790208)

Idaho National Engineering & Environmental Laboratory  
Lockheed Martin Idaho Technologies Company  
P.O. Box 83415  
Idaho Falls, Idaho 83415

INEEL Project Leader:  
S. M. Sorensen (208-526-9662)

NACHI Machining Technology Company  
17500 Twenty-Three Mile Road  
Macomb, Michigan 48044

NACHI Project Leader:  
Frances J. Wisner (810-263-0142)

National Research Council Canada  
Industrial Materials Institute  
75 de Mortagne  
Boucherville, Quebec, J4B 6Y4, Canada

IMI Project Leader:  
Guy Lamouche (450-641-5106)

Oak Ridge National Laboratory  
Instruments and Controls Division  
P.O. Box 2008  
Oak Ridge, Tennessee 37831

ORNL Project Leader:  
C. Ray Brittain (423-574-8949)

Sandia National Laboratories  
Materials and Processes Center  
P. O. Box 5800  
Albuquerque, New Mexico 87185

SNL Project Leader:  
J. Bruce Kelley (505-845-3105)

Scientific Forming Technologies Corporation  
5038 Reed Road  
Columbus, Ohio 43220

SFTC Project Leader:  
Wei-Tsu Wu (614-451-8330)

Synaps, Inc.  
2957 Clairmont Rd – Suite 170  
Atlanta, Georgia 30329

Synaps Project Leader:  
Alexander Van der Velden (404-320-7283)

The University of British Columbia  
Advanced Materials & Process Engineering Laboratory  
Room 111 - 2355 East Mall  
Vancouver, British Columbia, V6T 1Z4, Canada

UBC Project Leader:  
Mary A. Wells (604-822-1918)

**Additional Project Team Members** (Other contact information available upon request)

The Timken Company  
Canton, Ohio

AGH Krakow – University of Mining & Metallurgy  
Krakow, Poland

Case Western Reserve University  
Cleveland, Ohio

Central Iron & Steel Research Institute  
Beijing, China

DaimlerChrysler Corporation  
Detroit, Michigan

EB Scientific Enterprises  
Golden, Colorado

Engel Metallurgical, Ltd.  
St. Cloud, Minnesota

Gas Technology Institute  
Des Plaines, Illinois

Harbin Institute of Technology  
Harbin, China

InductoHeat  
Madison Heights, Michigan

The Ohio State University  
Columbus, Ohio

The Osada State Tube Institute  
Dniepropetrovsk, Ukraine

QuesTek Innovations, LLC  
Chicago, Illinois

SHAPE  
Seoul, Korea

U.S. Steel Group/USX Corporation  
Monroeville, Pennsylvania

Verein zur Forderung der Umform- und  
Produktionstechnik Riesa e.V.  
Riesa, Germany

Yanshan University  
Quinghuangdao, China

Automotive Business Contact:  
Roger Ellis

UMM (ELROLL) Contact:  
Maciej Pietrzyk

CWRU Contact:  
Gary Michal

CISRI Contact:  
Zhengdong Liu

DaimlerChrysler Contact:  
Eric McCarty

EB Contact:  
Elliot Brown

Engel Contact:  
James Brusso

GTI Contact:  
Harry Kurek

HIT Contact:  
Jitai Niu

InductoHeat Contact:  
Valery Rudnev

OSU Contact:  
Ragiv Shivpuri

DTI-VNITI Contact:  
Gennady Gulyayev

QuesTek Contact:  
Charles Kuehmann

SHAPE Contact:  
Juyoung Lee

USS Contact:  
Matt Merwin

VFUP Riesa Contact:  
Frank Gerlach

YSU Contact:  
Chao Zhou

## List of Abbreviations

| <u>Acronym</u> | <u>Definition</u>   |
|----------------|---|
| DOE            | U.S. Department of Energy   |
| DCAA           | Defense Contract Audit Agency   |
| VIPERS         | Vendor Inquiry Payment Electronic Reporting System  |
| ASAP           | Automated Standard Application for Payments System  |
| EF             | The Timken Company's office of External Funding   |
| <br>           |   |
| AISI           | American Iron & Steel Institute   |
| ASTM           | American Society for Testing of Materials   |
| SAE            | Society of Automotive Engineers   |
| MS&T           | Materials Science & Technology  |
| AIST           | Association of Iron & Steel Technology  |
| MMMS           | Minerals, Metals & Materials Society  |
| IWASPNDDE      | International Workshop for Advances in Signal Processing for<br>Non-Destructive Evaluation of Materials |
| <br>           |   |
| TMP            | Thermo-Mechanical Processing  |
| CCT            | Continuous Cooling Transformation   |
| TTT            | Time Temperature Transformation   |
| IF             | Interstitial-Free Steel   |
| FCC            | Face Centered Cubic   |
| M/A            | Martensite/Austenite  |
| JMAK           | Johnson-Mehl-Avrami-Komologrov Equation   |
| AlN            | Aluminum Nitride  |
| OCTG           | Oil Country Tubular Goods   |
| <br>           |   |
| HSMM           | Hot Strip Mill Model  |
| CTMP           | Controlled Thermo-Mechanical Processing   |
| TOM            | Tube Optimization Model   |
| VPP            | Virtual Pilot Plant   |
| LUT            | Laser-Ultrasonic Tube Gauge   |
| REML           | Robotically-Enhanced Manufacturing Line   |
| <br>           |   |
| AFC            | Advanced Final Cooling  |
| CR             | Controlled Rolling  |
| ESA            | Enhanced Spheroidize Annealing  |
| T-ESA          | Thermal Enhanced Spheroidize Annealing  |
| D-ESA          | Deformation Enhanced Spheroidize Annealing  |
| NEQ            | Normalize Equivalent  |
| ILQ            | Inline Quenching  |
| CSC            | Controlled Slow Cool  |
| <br>           |   |
| DoX            | Design of Experiments   |
| CI             | Continuous Improvement  |
| GUI            | Graphic User Interface  |
| FE             | Finite Element  |
| FD             | Finite Difference   |
| CMM            | Coordinate Measuring Machine  |

## **List of Abbreviations (continued)**

| <b><u>Acronym</u></b> | <b><u>Definition</u></b>    |
|-----------------------|-----------------------------|
| Btu                   | British Thermal Units       |
| HTC                   | Heat Transfer Coefficient   |
| IHC                   | Inverse Heat Conduction     |
| ISV                   | Internal State Variable     |
| <br>                  |                             |
| KRM                   | Kocks Rolling Mill          |
| PSM                   | Kocks Precision Sizing Mill |
| <br>                  |                             |
| OD                    | Outside Diameter            |
| ID                    | Inside Diameter             |
| 2-D                   | Two-Dimensional             |
| 3-D                   | Three-Dimensional           |
| <br>                  |                             |
| SFM                   | Surface Feet per Minute     |
| <br>                  |                             |
| PC                    | Personal Computer           |

# PROJECT OVERVIEW

## EXECUTIVE SUMMARY

The Alloy Steel Business of The Timken Company answered a competitive solicitation and won an award in September 1999 for the Controlled Thermo-Mechanical Processing (CTMP) project having assembled an impressive group of worldwide experts to serve as subcontracting partners, contractors and consultants. As proposed, the ambitious \$83 million five-year project included an R&D phase to be followed by a technology demonstration via deployment of equipment and processes in a new tube mill.

The premise of the CTMP work was to combine Timken's product understanding with its process expertise and knowledge of metallurgical and deformation fundamentals developed during the project to build a predictive process design capability. The project, a logical extension of the Hot Strip Mill Model (HSMM) project done by an American Iron & Steel Institute (AISI) consortium of steel companies with co-funding by the DoE, took advantage of advances in computing hardware and modeling science. A strong international public-private partnership was employed to advance the CTMP project toward its ultimate goal of real-time control of the tube making process. Process recipes were developed using this predictive capability to achieve targeted energy savings from improved efficiency and reduced scrap and rework. Recipes, as well as recommendations from other studies, have been successfully implemented.

Conditional approval was given for the project's future phases based on successful development of the models and associated predictive tools. Proposals for each of the three subsequent project years were approved, although the scope was altered in some cases due to business circumstances. As added tubing capacity was not a Timken business priority, the development of the planetary elongator coupled to the stretch reducing mill for demonstration in a new mill was concluded with the completion of the deformation model and the effort with Kocks was ended. The mill demonstration was replaced as a project task by the development of a Virtual Pilot Plant (VPP) feature. That tool would allow process and equipment scenarios to be evaluated in computer simulations, rather than using production facilities.

The CTMP effort succeeded in delivering a PC-based capability in the Tube Optimization Model (TOM) with the VPP of representing the desired tube making process to predict the resultant microstructure. Laboratory experiments and instrumented simulations were key tools in confirming the models and developing predictive algorithms. The results were verified by showing a close correlation of predicted to the recorded values in temperature studies and by the agreement of the microstructures with those predicted in selected base grades. The TOM and VPP combination offer great cost and energy savings potential in design of new plants or the optimization of existing or development of new process recipes.

A graphical user-friendly interface (GUI) has been developed for TOM to allow the user to setup the tube making process and to design the CTMP process easily on the computer. Features were included in TOM to allow the user to add other SAE-designated grades to the system either by incorporating published characterizing or empirical metallurgical data, or by altering data already in the system's database. An optimization capability was included to allow the user to investigate processes or alternatives under restrictions on processing parameters, economics, or other factors. The TOM and its capabilities have been fully documented.

Modeling enhancements have been created to make the TOM a more versatile product. The TOM uses FE or FD modeling to represent thermal and deformation effects. The microstructure evolution is based on 2-D FE models, which could be executed faster than 3-D models that were reserved for dimensional studies. Other capabilities, including a grain-size predictor, were developed to allow the user efficiently to explore the effects of processing parameter variation along the tube making process line.

Baseline grades were selected for study during the CTMP project, including a low-carbon bearing grade, an automotive gear steel, and a through-hardened bearing grade. The project tasks, including the metallurgical characterization and model development, were done for each of the grades. Additional grades for other applications, including some special Timken grades, were studied to broaden the correlations and the robustness of the models. The TOM product for commercialization will include the models and a library of the base and general grades as well as some literature data, but not the data from the special Timken grades. A commercialization plan is being developed with engineering and software vendors for the various products derived from the project. Timken may release non-competitive pieces before expiration of the three-year exclusive use period.

A number of successful recipes have been developed during the CTMP project. One highlight has been the development of a recipe for automotive gear steels referred to as the Advanced Final Cooling (AFC) process. A key element was the development of a verified surrogate test for gear cutting. Data generated from that product response test challenged Timken's previous understanding and led to the identification of the optimum structure. The TOM was then used to develop a robust recipe that was effective over a range of tube sizes. Efforts are underway to validate the improved performance of that product in the automotive manufacturers plants, and hence, to facilitate capture of the tooling cost savings.

Another project highlight was the work done on Enhanced Spheroidize Anneal (ESA) processes for high carbon, so-called through-hardened bearing steels. Two versions of the process have been explored. One process (D-ESA) uses on-line deformation to achieve an industry standard microstructure. The process was conceptualized, but not studied extensively because of equipment limitations. The other version, T-ESA, uses special thermal sequencing to reduce post processing heat treatment normally used to achieve the desired structure. The T-ESA process was implemented in production midway through the project.

During the later portion of the CTMP project, Timken's focus for cost reduction was on continuous improvement (CI) efforts. As the CTMP tools were developed, they were applied to several of these CI studies. One example was FE model of the reduction mill that was used to optimize the roll pass sequence for best dimension control with fewest defects. Several process changes were implemented.

Other capabilities were investigated to complete the concept of modeling the response as well as the processing. In particular, a model from first principles for turning was attempted using FE concepts. Although the development succeeded in producing a representation of the process, the correlation was not sufficient to merit further investigation.

A task was included in the CTMP project to perform direct, on-line measurement of the austenitic grain size. That task exploited the successful laser-ultrasonic tube wall and eccentricity gauge (LUT) project done by Timken with DoE co-funding under Award #DE-FC07-99ID13651. Development efforts in the CTMP project, using a signal attenuation approach and parallel data processing, succeeded in delivering a grain size measurement capability for each tube that met targeted accuracy specifications without interfering with the wall measurements.

Late in the project, a task was added to demonstrate the deployment of CTMP concepts in a Robotically Enhanced Manufacturing Line (REML) for the efficient production of small lots of tapered roller bearings. Two important concepts for investigation were robotics to enable advanced manufacturing concepts and remove repetitive manual labor, and alternate, on-demand heating techniques for greater efficiency. In addition, the robotic development will look for opportunities to reduce cost and save energy by advancing the area of "lightweight robotics". In the first phase of the project, equipment was acquired and installed in a process line for later capability studies and optimization. The TOM will be used to explore the best tube product condition as an input to the REML.

## FOREWORD

The U.S. Department of Energy (DoE) co-sponsored the CTMP project, with Timken agreeing to provide a minimum 30% cost share. Mr. Isaac Chan and Mr. Simon Friedrich monitored the project at DoE Headquarters in Washington D.C. Dr. Gideon Varga, the LUT program manager, is acknowledged for supporting the system's use for CTMP research. The project initially was administered by DoE's Idaho Operations Office with Mr. Robert G. Trimberger acting as project manager and Ms. Elizabeth E. Dahl serving as award specialist. The administration was transferred in 2003 to the Golden Field Office where Dr. Dibyajyoti (Debo) Aichbhaumik became project manager and Ms. Jean M. Siekerka served as the award specialist. Payments originally were made from the Albuquerque Office and later from the Oak Ridge Office.

Timken's visionary for the marriage of technologies into the CTMP project was Mr. Erich D. Dominik, who initiated the project effort and served as its executive sponsor until his retirement. Dr. Raymond V. Fryan succeeded Mr. Dominik in the sponsor's role and provided project direction through its conclusion. Dr. Robert V. Kolarik II served as Timken's project manager during the project.

The CTMP project plan was structured into a number of subtasks – each with its own technical lead. The key subtask leaders are listed below:

- Mr. Jeffery E. Ives - Thermal-Deformation Fundamentals
  - Mr. E. F. (Buddy) Damm - Metallurgical Characterization
  - Dr. Daqing Jin - Process Modeling
  - Mr. Michael E. Burnett
  - Mr. Craig V. Darragh
  - Mr. Robert H. Vandervaart
  - Mr. Gerald V. Jeskey – Direct Measurement
- } Product Response

Mr. Ives also served as assistant project manager.

Other Timken technical staff members supporting project subtasks included Mr. Steven E. Agger, Dr. James A. Brusso, Mrs. Guizhen (Jane) Chen, Mr. Michael L. Mester, Mr. Thomas L. Misanik, Mr. Anthony J. Perez, Dr. Krich Sawamiphakdi, Mr. J. Darrel Yingling and Dr. John C. Wei.

Ms. Jo Ann Klingaman, Ms. Hua (Barbara) Guo and Mr. Bruce Calvin played significant roles in administration during the project's early years. At the conclusion of the project, its administration fell under the purview of the newly formed Timken External Funding Office.

The CTMP project was supported by a capable group of engineers and technicians from Timken's Alloy Steel Business and at Timken Research. An advisory committee of managers served as a steering committee and reviewed project progress and addressed issues on a monthly basis. Quarterly reports were provided to the senior management team of the Steel Business.

A group of expert consultants and contractors from various research organizations and national laboratories including those listed behind the title page rounded out the CTMP project team. Each of those resources performed its tasks well and is to be commended for its cooperation and hard work.

Several of the proposed partners did not participate in the CTMP project. The U.S. Steel Group withdrew because plant support for the model waned as contracts were being negotiated. The Ford Motor Company and DaimlerChrysler Corporation each provided advice on product targets for automotive gear steels, but only limited acceptance tests were conducted during the project. In an extension to those limited tests, DaimlerChrysler has begun to evaluate material outside the project.

## TABLE OF CONTENTS

|  |      |
|--|------|
| 1) Project Overview  | i    |
| a) Project Team Members  | ii   |
| b) Additional Project Team Members                                 | iv   |
| c) List of Abbreviations   | v    |
| d) Executive Summary   | vii  |
| e) Foreword  | viii |
| f) Table of Contents   | x    |
| g) List of Figures   | xiii |
| h) List of Tables  |      |
|  |      |
| 2) Introduction  |      |
| a) Capability Building   | 1    |
| b) Tube Making Process   | 2    |
| c) Technical Barriers  | 3    |
| d) Analytical Tools  | 3    |
| e) Benefits  | 4    |
|  |      |
| 3) Task 1 - Project Management                                     | 6    |
|  |      |
| 4) Task 2 – R & D Subtasks   | 8    |
|  |      |
| a) Subtask 2.1 – Deformation and Heat Transfer – Fundamental Study | 10   |
|  |      |
| b) Subtask 2.2 - Metallurgical Characterization                    |      |
| i) Metallurgical Models Overview                                   | 13   |
| ii) Metallurgical Model Development                                | 13   |
| (1) Grain Growth   | 13   |
| (2) Recrystallization  | 14   |
| (a) Phenomenological Approach                                      | 14   |
| (3) Monte Carlo Potts Model Approach                               | 16   |
| (4) Flow Stress  | 18   |
| (a) Phenomenological Approach                                      | 18   |
| (b) Internal State Variable (ISV)                                  | 20   |
| (5) Austenite Decomposition  | 21   |
| (a) Internal State Variable (ISV)                                  | 21   |
| (b) QuesTek MCASIS   | 22   |
| (c) CCT-TTT Curves   | 22   |
| (6) Theoretical Thermal Expansion Coefficients                     | 23   |

## TABLE OF CONTENTS (continued)

|  |    |
|--|----|
| Subtask 2.3 - Process Modeling                                       |    |
| iii) Objectives  | 26 |
| iv) Development of Process Models                                    | 26 |
| v) Tube Optimization Model (TOM)                                     | 26 |
| (1) Introduction   | 27 |
| (2) Piercing Mill Model  | 27 |
| (3) Assel Elongating Mill Model                                      | 29 |
| (4) Reducing Mill Model  | 29 |
| (5) Stretch Reducing Mill Model                                      | 30 |
| (6) Induction Heating Model  | 31 |
| (7) Quenching/Rapid Cooling Model                                    | 32 |
| (8) Controlled Slow Cooling (CSC) Model                              | 32 |
| (9) Material and Metallurgical Models/Database                       | 33 |
| (a) Steel Chemistry  | 33 |
| (b) Thermal Physical Properties                                      | 33 |
| (c) Flow Stress  | 33 |
| (d) Recrystallization and Grain Growth                               | 34 |
| (e) Transformation Model   | 34 |
| (10) Tooling and Production Scheduling Module/Database               | 34 |
| (11) Optimization Module   | 36 |
| (12) User-Friendly Graphics Interface (GUI)                          | 36 |
| (13) Virtual Pilot Plant (VPP)                                       | 37 |
| (14) Verification of TOM   | 37 |
| vi) 2-D FE Analysis  | 38 |
| (1) FE Formulations and Algorithms                                   | 38 |
| (2) Mannesmann Piercing Mill   | 39 |
| (3) Assel Elongating Mill  | 41 |
| (4) Planetary Elongating Mill  | 43 |
| (5) Radial Forging Process   | 44 |
| (6) ABAQUS™ - Explicit FE Analysis                                   | 46 |
| (7) Straightening Mill   | 46 |
| (8) SHAPE™ for Simulation of Reducing and Stretch Reducing Processes | 50 |
| (9) TubeRoll Program   | 50 |
| (10) Reducing Mill   | 50 |
| (11) DEFORM™ for Simulation of Machining Processes                   | 54 |
| vii) Application of Process Modeling Tools                           | 55 |
| c) Subtask 2.4 – Process Simulation                                  | 56 |

## TABLE OF CONTENTS (continued)

|  |    |
|--|----|
| d) Subtask 2.5 - Process Verification                      |    |
| i) Process Recipes   | 57 |
| (1) Advanced Final Cooling (AFC)                           | 57 |
| (2) Controlled Rolling (CR)                                | 60 |
| (3) Thermal Enhanced Spheroidized Annealing (T-ESA)        | 60 |
| (4) Deformation-Enhanced Spheroids Annealing (D-ESA)       | 61 |
| ii) Normalize Equivalent (NEQ)                             | 63 |
| (1) Lab Studies  | 63 |
| (2) Mill Trials  | 65 |
| iii) Inline Quenching                                      | 66 |
| e) Subtask 2.6 - Product Response                          |    |
| i) Bearing Business Product Response Tests                 | 70 |
| (1) Screw Machine Test                                     | 71 |
| (a) Test Description                                       | 71 |
| (b) Test Results   | 71 |
| (2) Turning Test   | 71 |
| (a) Test Description                                       | 71 |
| (b) Test Results   | 71 |
| ii) Automotive Customer Product Response Tests             | 72 |
| (1) Broach Test  | 73 |
| (a) Test Description                                       | 73 |
| (b) Test Results   | 75 |
| (c) Validation Testing                                     | 75 |
| f) Subtask 2.7 - Direct Measurement                        |    |
| i) Application of LUT as Grain Size Sensor                 | 76 |
| ii) Laser-Ultrasonics to Monitor Microstructure            | 79 |
| iii) LUT Configuration for Gleeble System                  | 80 |
| g) Subtask 2.8 – Controls                                  | 82 |
| 5) Task 3 – Pilot Plant                                    | 84 |
| 6) Task 4 – Plant Trials                                   | 84 |
| 7) Task 5 - Robotically Enhanced Manufacturing Line (REML) |    |
| a) Subtask 5.0 – Order and Delivery of Equipment           | 85 |
| i) Green Cell  | 85 |
| ii) Thermal Treatment Cell                                 | 86 |
| iii) Finish Cell   | 87 |
| b) Subtask 5.1 – Energy Savings Model Task                 | 88 |
| c) Subtask 5.2 – Tube Optimization Model (TOM) Task        | 88 |
| 8) Reference List  | 89 |

## List of Figures

| <b><u>Number</u></b> | <b><u>Caption</u></b>  | <b><u>Page</u></b> |
|----------------------|--|--------------------|
| 0-1                  | Timken's Global Technology Stream vision   | 1                  |
| 0-2                  | Vision of the impact of the CTMP project   | 2                  |
| 0-3                  | Process flow of tube making  | 2                  |
| 2.1-1                | Comparison of CSC model to measured results  | 10                 |
| 2.1-2 a              | Rig spray test at UBC – Hot tube segment   | 11                 |
| 2.1-2 b              | Rig spray test at UBC – Spray in progress  | 11                 |
| 2.2-1                | Modeled versus measured grain coarsening kinetics example  | 14                 |
| 2.2-2                | Modeled versus measured recrystallization kinetics example   | 17                 |
| 2.2-3                | Monte Carlo time step versus "grain size" in the presence of<br>Zener-pinning particles or ALN   | 18                 |
| 2.2-4                | Modeled versus measured flow stress examples   | 20                 |
| 2.2-5                | ISV transformation model predictions for phase fraction as a function<br>of cooling rate and prior austenite grain size for 5130 steel | 22                 |
| 2.2-6                | Interface to chemistry based CCT/TTT modeling.   | 23                 |
| 2.2-7                | Example of measured and modeled dilation data and the resulting<br>phase fractions as determined by the ISV transformation model       | 25                 |

## List of Figures (continued)

|          |   |    |
|----------|---|----|
| 2.3-1    | TOM GUI   | 27 |
| 2.3-2    | Piercing mill model setup   | 28 |
| 2.3-3    | Example of results from piercing process simulation   | 28 |
| 2.3-4    | Assel elongating model setup  | 29 |
| 2.3-5    | Reducing mill model setup   | 30 |
| 2.3-6    | Stretch-reducing mill setup   | 31 |
| 2.3-7    | Induction heating model application   | 31 |
| 2.3-8    | Induction heating model predictability  | 32 |
| 2.3-9    | Steel grade database  | 33 |
| 2.3-10   | Flow stress database GUI  | 33 |
| 2.3-11   | Recrystallization and grain growth GUI  | 34 |
| 2.3-12   | Production scheduling GUI   | 35 |
| 2.3-13   | Tooling design GUI  | 35 |
| 2.3-14   | Optimization GUI  | 36 |
| 2.3-15 a | Thermal history and microstructure evolution of seamless tubing during a conventional hot rolling process | 38 |
| 2.3-15 b | Thermal history and microstructure evolution of seamless tube during a cooling process                    | 37 |
| 2.3-16   | FE models of piecing, Assel elongating and planetary elongating process                                   | 39 |
| 2.3-17   | Typical Mannesmann piercing mill  | 40 |
| 2.3-18   | Analysis results of piercing process  | 40 |
| 2.3-19   | Typical system of Assel elongating mill   | 41 |
| 2.3-20   | FE model of Assel elongating process  | 42 |
| 2.3-21   | Deformation of tube along the elongating mill   | 42 |
| 2.3-22   | Cross-sections along the forming axis at different locations  | 42 |
| 2.3-23 a | Contour of strain rate  | 43 |
| 2.3-23 b | Profile of forming load   | 43 |
| 2.3-24   | FE model of planetary elongating process  | 44 |
| 2.3-25   | Schematic of radial forming process   | 45 |
| 2.3-26   | FE model of radial forging process  | 45 |
| 2.3-27 a | Strain distribution in the billet   | 46 |
| 2.3-27 b | Temperature distribution in the billet  | 46 |
| 2.3-28   | FE models of straightening and Assel elongating processes   | 46 |
| 2.3-29   | Typical two-roll straightening mill   | 47 |
| 2.3-30   | Typical five-roll straightening mill  | 47 |
| 2.3-31   | FE model of two-roll straightening process  | 48 |
| 2.3-32   | FE model of five-roll straightening process   | 48 |
| 2.3-33   | Contact loads from two-roll straightening   | 49 |
| 2.3-34   | Contact loads from five-roll straightening  | 49 |
| 2.3-35   | Illustration of dual-meshing technique  | 50 |
| 2.3-36   | FE model of reducing mill   | 51 |
| 2.3-37 a | Analysis results of reduced tube – Contour of temperatures  | 51 |
| 2.3-37 b | Analysis results of reduced tube – Contour of residual stresses   | 51 |
| 2.3-38   | Comparison of wall variation due to different reduction pass design                                       | 52 |
| 2.3-39   | Typical set up of reducing and stretch reducing mills   | 53 |
| 2.3-40   | Analysis results of 18-station stretch reducing mill  | 53 |
| 2.3-41   | Comparison of analysis and actual geometries after Station No. 18   | 53 |
| 2.3-42   | Representation of machining modeling  | 54 |

## List of Figures (continued)

|         |   |    |
|---------|---|----|
| 2.4-1   | Plant rapid cooling device  | 56 |
| 2.5-1   | Comparison of laboratory quench profiles at different tube locations to thermal profiles applied in Gleeble dilatometry investigations for the AFC process                          | 58 |
| 2.5-2   | Dilation versus temperature curves for two AFC simulations and one full quench (to identify the martensite transformation temperature)  | 59 |
| 2.5-3   | Dilation versus time for the AFC simulations shown in Figure 2.5-2  | 59 |
| 2.5-4 a | Uniform microstructure produced by 10-hour T-ESA cycle  | 60 |
| 2.5-4 b | Uniform microstructure produced by 16-hour T-ESA cycle  | 60 |
| 2.5-5   | D-ESA microstructure  | 62 |
| 2.5-6   | Tube making physical simulation of the NEQ process using the Gleeble torsion thermo-mechanical process simulator  | 64 |
| 2.5-7   | Torque versus torsion (similar to stress versus strain) curves for tube making physical simulation of the NEQ process using the Gleeble torsion thermo mechanical process simulator | 64 |
| 2.5-8   | Grain size versus sink temperature for a series of steels and sink amounts derived from NEQ simulations using the Gleeble torsion thermo-mechanical process simulator               | 65 |
| 2.5-9   | Conventionally normalized 1045  | 66 |
| 2.5-10  | NEQ processes 1045 (OD)   | 66 |
| 2.5-11  | Hardness versus tempering temperature for 4130 subject to a range of processing paths   | 67 |
| 2.5-12  | Rotating bending fatigue data for 4130 direct quenching investigation   | 67 |
| 2.5-13  | Charpy impact data for 4130 direct quench investigation   | 68 |
| 2.5-14  | Strength and ductility variation as a function of tempering temperature and total reduction   | 69 |
| 2.6-1   | Broach cutting  | 72 |
| 2.6-2   | Structure of a broach bar   | 72 |
| 2.6-3   | Typical automotive ring gear  | 73 |
| 2.6-4 a | Broach test machine and control stand   | 74 |
| 2.6-4 b | Close-up of part manipulation table and coolant lines   | 74 |
| 2.6-5   | Broach tool showing three cutting teeth   | 74 |
| 2.6-6   | Test ring with a broach tool shown in cutting position  | 74 |
| 2.7-1 a | Principle of laser-ultrasonic generation and detection in a tube  | 76 |
| 2.7-1 b | Signal acquired on-line for a 16 mm thick tube at 940 C   | 76 |
| 2.7-2   | Overview of the laser ultrasonic system   | 77 |
| 2.7-3   | Calibration between the fitted attenuation parameter “b” and the austenitic grain size from metallography   | 78 |
| 2.7-4   | Grain size measured on-line by the LUT system and measured by metallography after proper quenching  | 79 |
| 2.7-5   | Schematic description of the system proposed by IMI   | 80 |
| 5-1     | Comparison of energy consumption of REML line versus current process baseline   | 88 |

## List of Tables

| <u>Number</u> | <u>Title</u>                              | <u>Page</u> |
|---------------|---|-------------|
| 2.2-1         | Number of substantial atoms per unit cell | 24          |
| 2.6-1         | Broach test validation                    | 75          |

# INTRODUCTION

## Capability Building

The Timken Company's technology management team recently developed a model to explain its role in the Company's global technology stream (Figure 0-1). The model shows the flow of ideas and concepts originating in science, developing via technology, being practiced through engineering, growing to application, expanding by proliferation, leading to commercial value in product sales. The role of the Technology Center is to develop capabilities converting science into technology which can be exploited to manufacture products that are differentiated by such characteristics as better performance and superior properties, or lowest price or reduced energy content.

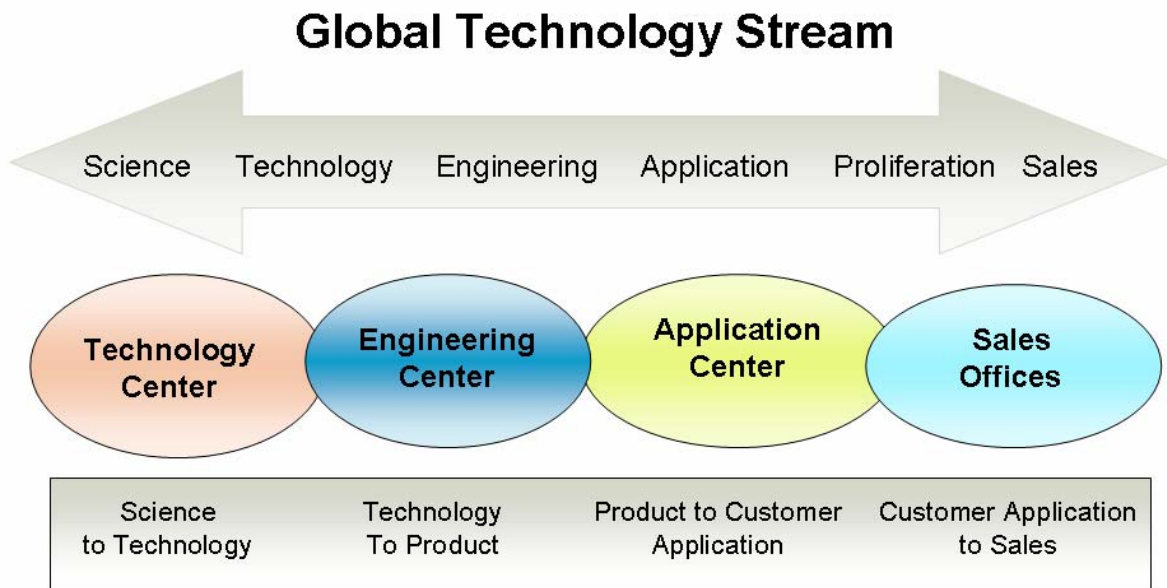


Figure 0-1. Timken's Global Technology Stream vision.

The CTMP project is an excellent example of that capability building. The concept advanced in this project began with the claim that the behavior of steel tube or pipe product can be well enough understood or characterized to suggest a preferred or optimum microstructure and associated concomitant properties for an intended application. Further, with the metallurgy, deformation and thermal sciences sufficiently well understood, modeling and computational technology could be exploited to develop a model of the selected process. That model would then be applied to tailor the process to meet desired specifications.

The vision of the CTMP project is illustrated in the railcar analogy shown in Figure 0-2. At the outset of the CTMP project, the tube making resources owned by the domestic producers generally had limited capabilities which typically resulted in product with relatively high variation and provided little capability for control. Application of CTMP was envisioned to enable consistent products to be made with targeted structure and properties. The improved control and less variable properties would result in improved performance in customer applications such as machining. Not only could the response be maximized, the process could be tailored to deliver that same benefit to a specific plant or process conditions as represented by the shifting of the railcar.

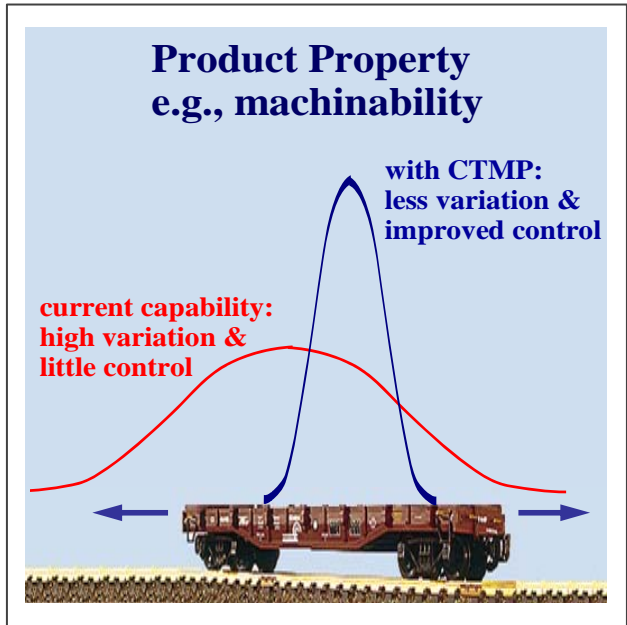


Figure 0-2. Vision of the impact of the CTMP project.

### Tube Making Process

The CTMP project dealt with the technical aspects of the production of seamless mechanical steel tubing. The general process flow for tube manufacture is shown in Figure 0-3. The billet is pierced by the cross-rolling action of barrel-shaped rolls. A mandrel bar inside the hollow helps to form the desired inner diameter. The hollow proceeds to the elongator where the deformation of three skewed rolls forms and elongates the hollow into a shell with the desired wall thickness. After a temperature adjustment by cooling and/or heating, the outside diameter is reduced to the aim size by a series of perpendicularly-oriented rolls. The tube is rounded to final size and shape by a rolling operation at the rotary sizer. The tube is rounded to final size and shape by a rolling operation at the rotary sizer.

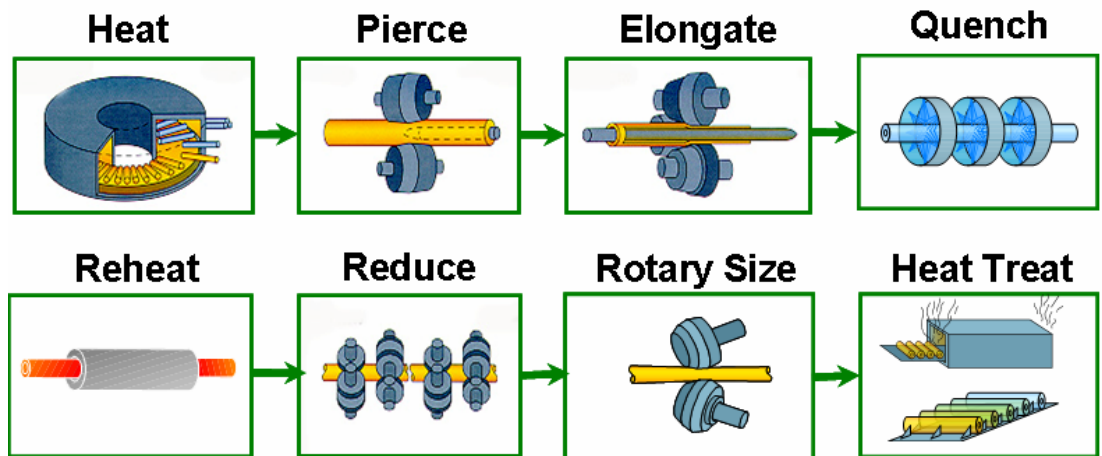


Figure 0-3. Process flow of tube making.

## Technical Barriers

The following were identified as significant barriers to be overcome during the project's R&D phase:

- Characterization of the effect of retained strain on austenite decomposition, requiring special thermo-mechanical testing,
- Characterization of the effect of low-temperature rolling on the cycle time for ESA, which will require specially designed equipment for low temperature rolling,
- Precise deformation rates, which will require revolutionary equipment and control,
- Precise, uniform temperatures during processing, which will require development of a unique cooling device with sophisticated control,
- On-line determination of austenite grain size, which will require development of a direct measurement sensor,
- Integrated system control, which will require sophisticated control of the equipment and devices with input from the model and sensors.

These hurdles, as well as many others encountered during the project, were solved or overcome during the course of the project.

As the CTMP project progressed, it became clear that the team was going to be successful in developing verified tools. However, developing the tools was just a means to an end, with one very important end being the creation of process recipes resulting in product with commercial value. During the course of the project, Mr. Roger Kisner of ORNL coined the term "trajectory". That term appropriately describes the concept that there is a target process path to achieve the desired end, but one that allows some variation and can accommodate correction guided by the appropriate process controls.

## Analytical Tools

Timken's process team demonstrated command of many analytical tools to assist in the technical development. One such tool is the Design of Experiments (DoX) methodology. Application of DoX facilitates efficient investigation of relationships between controllable factors in a manufacturing process and key customer qualities. In the CTMP program, DoX was used in several of the study areas, including the metallurgical characterization and process recipe development, as well as in verification studies.

The issues in these studies were complex and required controlled analytical approaches. The DoX approach accomplishes this efficiently as designs are based on the objective (e.g., factor reduction, ranking, and/or optimization) and allow for balancing the cost of experimentation versus the expected information to be gained. Each of the DoX's involved extensive planning. Most important was determining how to minimize the effect of non-factors so that the most important factors could clearly be determined. This was accomplished by blocking, role assignments, dry runs and contingency planning.

The results of the CTMP trials and the efficient development of ultimately effective tools were proof of the power of DoX. In virtually all trials, key factors were identified and real production practices developed and implemented. This has resulted in better machining (8119 study), quicker heat treat (ESA development), more consistent grain structure (grain size prediction), and quicker product development (broach screening). Application of the DoX greatly improved the efficiency of the project investigations and provided value to Timken and the DoE.

The information learned has also been programmed into the optimization feature included in TOM. The optimization approach allows the user to value the cost and properties to seek the most robust solution. The results accomplished on the CTMP project and the capabilities represented in TOM could not have been accomplished without the efficient and robust approach of DoX.

## Benefits

In recent years, there has been some debate between the steel industry, led by progressive companies such as Timken, and the DoE on the subject of benefits. Certainly, the industry recognizes the DoE's mission to reduce energy consumption, while positively impacting the environment and increasing efficiency leading to increased competitiveness of U.S. industry. However, the steel industry resists the "inside the steel plant fences" limiting view for quantifying savings and maintains that the sphere of influence should be defined much as the companies must do from a business perspective, considering the performance of their product and its life cycle.

Benefits to the customer ultimately are benefits to the steel company. While efforts to predict product performance were endorsed by DoE, counting the downstream impact of savings attributable to the producer's technology development was not permitted. Timken contends that such holistic approaches should be encouraged as they would lead to the most beneficial projects to the country being funded. The following illustrate such broader potential benefits:

- material and manufacturing cost savings when product does not have to be replaced unexpectedly or sooner than anticipated,
- preserved production capacity when improved product performs better in the application - extending its life span,
- avoidance or minimization of engagement time of scarce technical resources to diagnose and solve often recurring customer problems,
- faster development time that preserves the customer's competitive advantage
- preserve tubing as a viable net shape material to lower overall energy content
- differentiated products that preserve U.S. steel markets.

The capabilities developed in this project should have many benefits to the tube and pipe segment of the steel industry and beyond, although the direct benefits accumulated within Timken's fences are somewhat limited to date. The project demonstrated that science developed into applicable technology can differentiate domestic products and further the cause of U.S. competitiveness in the global market.

While not represented in the proposal, the ability provided in TOM and the VPP to perform process and equipment design has huge, almost incalculable benefits. Those tools can assist in plant and equipment design with the potential to save initial or follow-on capital cost. With new plant costs in the tens of millions of dollars, one-time benefits from the application of VPP arguably could be in the single-digit millions of dollars. Decisions for added equipment could also be judged using these new tools, resulting in correct specifications for equipment to deliver the required capability with similar financial impact.

In the original project proposal, benefits were cited as coming from reductions in the following:

- alloy content required to make properties
- scrap and re-work in production
- post-processing heat treatments
- machining and tooling costs

Prior to the start of the CTMP project, Mr. Michael Burnett, a Timken scientist, proposed that microstructure manipulation and control could be used to deliver the properties needed for enhanced performance previously accomplished through additional alloying. That notion was proven to be correct during the project when a desired response in automotive gear steels was attained. Considerable benefit can be derived in savings from avoiding additional alloying at a time of relatively high alloy prices and from the environmental impact from the reduced demand for alloys. Again, such cost avoidance benefits are difficult to estimate, but they would be significant and would grow over time.

Process and product development work can now be done via the computer, and experimentation need only be done in the plant to verify and validate results. While impact of the new tools on product development activity is difficult to assess, an estimate was prepared assuming four production heats were necessary to conduct a test program, but only one was needed by applying TOM. Energy values were compiled using the DoE's Energy Intensity values [Ref 0]. Assuming three, 100-ton heats would have been melted and 25% of the material processed into tubes, approximately 0.7 billion Btus would be saved. Of course, the associated benefits of material savings and reduced greenhouse gas emissions would be gained as well.

The TOM provides tremendous opportunity for process studies without interrupting production. Such avoidance would have significant value in and of itself. A number of studies have been conducted at Timken during the final years of the CTMP project to take advantage of this new tool. Those studies also included dimensional control and defect elimination efforts. The accumulated annual savings are estimated at nearly \$1 million, not to mention the opportunity cost that the tools provided by reducing the time that would be required of the technical staff to execute those studies without TOM. The success of those efforts has provided short-term cost reduction, but perhaps more importantly has preserved tubing as a material of choice for those customer applications. It has also enriched the knowledge of Timken's technical staff that likely will lead to future technical or production benefits as those individuals continue their careers.

The primary goal of process improvement activities is process elimination, but process cycle reduction can be an attractive target. An example of this is the ESA work conducted during the project. While the D-ESA version which would eliminate post-process heat treatment has proved initially capable, equipment limitations have prevented implementation of that process. However, the T-ESA version has been perfected and implemented accomplishing a 33-50% process reduction. Savings are dependent on the type of heat treat furnace used and the production level for the through-hardened material, but estimates are \$0.5 million on savings of 0.1 billion Btus annually.

The successful development of the broach screening test is noteworthy and the hope is that the test becomes a valuable tool in problem solving and product development. Timken experienced such an event when its scientists developed an ultrasonic tool to assess steel cleanness (non-metallic inclusion content) in the late 1970s, the results of which directly correlated to bearing fatigue life performance. That tool was a key to a rapid development of Timken's clean steel practices that drove the industry and resulted in improved materials with the associated benefits to product performance. The broach screening test could have such an impact if products with improved microstructures for gear cutting are developed.

From the initial results accumulated during the CTMP project, a new understanding of product response was gained and a preferred structure revealed. Those new results have only been optimized for a specific set of gear cutting conditions. The potential of the screening test is significant as the cutting tooling is nearly half the cost of a gear and the industry-wide savings offer a potential opportunity exceeding \$10 million annually. Armed with this new understanding and the validated test, new products may be forthcoming in rapid order, allowing the broach test to rank with the ultrasonic cleanness test in importance in Timken's technology history.

In summary, as proposed the CTMP project produced the capability to investigate and optimize the tube making process to achieve target metallurgical structures with consideration to process robustness and cost. The resulting tools, such as the TOM and the VPP with the tooling and steel grade databases, enabled the tools to be customized for application by any tube producer. Timken has already demonstrated successes by applying the tools to achieve dramatic savings from specific studies for energy and cost reduction and to probe new and improved products with great potential downstream benefits.

## TASK 1

### Project Management

The project management task included the usual work of tracking actual costs and monitoring progress versus the plan, and managing mitigating variances. In addition, it involved coordination between team members, compliance with procedure, and preparation of progress reports in DoE's format.

At the outset of the CTMP project, Timken had not yet established its External Funding (EF) Office and planned to rely on its best practices to manage the project. A strong team structure featuring an enthusiastic executive sponsor, an experienced project leader and technically accomplished subtask leaders was established to execute the project. A steering committee representing marketing, manufacturing and technology management was created and met monthly to direct the project's efforts. A senior management group from Timken's Alloy Steel Business and Technology Center received quarterly updates and set project direction based on business needs.

Administrative functions largely were accomplished by the project leader and assistant. At the initiation of the project, the labor rates were determined by the Business Economics Group working with Steel's Organizational Advancement leader and the Defense Contract Audit Agency (DCAA). Tracking of labor hours was seen as a system weakness by the DCAA, so a spreadsheet reporting and costing system was built by a Business Economics associate. Hours were entered either by the associates or by the assistant as reported by the associate, and were verified by the project leader. Timken's normal purchasing systems were used to track the project costs and used as inputs to an expenditure database and other spreadsheets in preparing invoices.

For the last portion of the project, tracking made use of the new tools and methodologies developed by the EF Office. Labor rates had been determined and approved by DCAA and the commercial package, Planview, was used for time keeping. A new invoicing spreadsheet was used to summarize charges. Coincidentally, invoicing changed from a manual system to the on-line DoE's Vendor Inquiry Payment Electronic Reporting System (VIPERS) to the Automated Standard Application for Payments System (ASAP) with the U.S. Treasury Department.

Shortly after the project was initiated, a patent waiver was applied for by Timken and granted by the DoE's Chicago Office. Several areas of investigation have merited protection, but to date only the following patent applications have been filed or are being pursued:

- "Optimization of Steel Metallurgy to Improve Broach Tool Life"  
- United States Provisional Application - No. 60/606,816 - filed September 2, 2004.
- "Method and System for Determining Material Properties using Ultrasonic Attenuation"  
- Canada and United States Provisional Application - No. 11/174,496 - filed July 6, 2005.
- To be filed – "Thermal Mechanical Process for Spheroidize Annealing of Steels"
- To be filed – "Elongator Controlled Rolling"

Acknowledging the negotiated three-year exclusive-use period granted by the DoE for technology developed under the CTMP product, Timken anticipated technology developments and defined ownership and deployment in its subcontracts and has begun the process of developing a commercialization plan. In some cases, the plan may be immediate release for sale, while for the more competitive items, availability may be delayed for the full three years. The major commercial product will be the TOM. Timken has begun talks on that subject with the agent commercializing HSMM software.

Other pieces of commercially valuable technology, such as the broach test, and modules such as the ISV transformation model, deformation-flow stress model and meso-scale Potts model, will be identified and appropriate actions taken. In particular, the grain size measurement capability already has been released and added to the LUT commercial package currently being marketed by Tecnar Automation Ltee.

A review process was created at Timken to consider publication requests. Because of commercial considerations, publication generally has been restricted throughout the project. The first subject released for publication was the grain size measurement method. That subject has been the topic of several papers as listed below.

- G. Jeskey, R. Kolarik, E. Damm, J.-P. Monchalain, G. Lamouche, S. E. Kruger and M. Choquet “Laser Ultrasonic Sensor for On-line Seamless Steel Tubing Process Control”, 16th World Conference on Nondestructive Testing, Montreal, August 30 - September 3, 2004.
- G. Jeskey, R. Kolarik, E. Damm, J.-P. Monchalain, G. Lamouche, S. E. Kruger and M. Choquet “Laser Ultrasonic Sensor for On-line Seamless Steel Tubing Process Control,” AIST 2004.

With the approval of the DoE, the capabilities of TOM and selected other technical developments were introduced to the public in presentations made at the Materials Science & Technology (MS&T)'04 Conference in New Orleans. That conference was co-sponsored by Association of Iron & Steel Technology (AIST) and Minerals, Metals & Materials Society (MMMS). Additional papers and presentations will be approved as release is warranted.

- R. V. Kolarik, C. V. Darragh, J. E. Ives, D. Q. Jin, E. Buddy Damm, M. E. Burnett, “Controlled Thermo-Mechanical Processing of Tube and Pipe for Enhanced Manufacturing and Performance,” AIST 2004.
- D.Q. Jin, E.F. Damm, J. E. Ives, A. J. Perez, K. Sawamiphakdi, R. V. Kolarik, “Tube Optimization Model – An Integrated Process Modeling and Optimization Tool for Seamless Tube Making,” AIST 2004.
- D. F. Li and M.A. Wells, “Accurate Temperature Measurement During Water Quench Operations Characterized by Boiling Water Heat Transfer,” AIST 2004.
- K. Sawamiphadki, D. Q. Jin, and A. J. Perez, “Overview of 3-D Finite Element Modeling in Tube Making Processes,” AIST 2004.
- D. Lévesque, S.E. Kruger, G. Lamouche, R. V. Kolarik II, G. V. Jeskey, M. Choquet and J.-P. Monchalain, “Thickness and grain size monitoring in seamless tube making process using laser-ultrasonics,” Fifth International Workshop in Advances in Signal Processing for Non Destructive Evaluation of Materials (IWASPNDE), 2-4 August, 2005, Université Laval, Quebec City, Qc, Canada.
- S.E. Kruger, G. Lamouche, R. V. Kolarik II, G. V. Jeskey, M. Choquet and J.-P. Monchalain, “On-line Monitoring of Wall Thickness and Austenite Grain Size on a Seamless Tubing Production Line at the Timken Company,” AISTech 2005, Iron & Steel Technology.

## TASK 2

### R&D Subtasks

The project's technical efforts were divided into subtasks managed by appropriately qualified Timken technical experts. The purpose of this task, performed mainly in laboratory settings, was to verify the CTMP concept, to build and verify the components needed to represent the tube and pipe making process, and to identify the desired microstructure that produces an improved response for the product user. Fundamental metallurgical studies were done, as was work to simulate the deformation processes under mechanical and instrumented test conditions. Work also was done to model the deformation, cooling and heating processes, to make important in-process measurements, and to calibrate those modules to measured responses.

The goals of the respective R&D Subtasks are summarized below:

#### **Subtask 2.1: Deformation and Heat Transfer - Fundamental Study**

Studies of heat transfer phenomena during the piercing, elongating and reducing processes and during the rapid cooling and heating processes were proposed to gain a better understanding for use in modeling and process control. Thermocouples were to be used during each process to measure the change of temperature and heat transfer. Mathematical models to calculate the heat transfer coefficients under various conditions were to be developed for process modeling. Rolling load and pressure during the piercing, elongating and reducing processes were to be studied for the purpose of deformation control at low temperature.

#### **Subtask 2.2: Metallurgical - Fundamental Study**

Microstructure evolution, final structure and properties can be defined through the precise control of thermal and mechanical deformation. Studies of recrystallization kinetics, grain growth, austenite decomposition kinetics, flow stress and their interactions under various thermal and deformation conditions were planned for selected steel grades in order to determine the state of metallurgical structure during the tube making process. Mathematical models were to be developed to characterize these behaviors and the thermal and deformation effects in developing the process conditions to produce the desired final microstructure.

#### **Subtask 2.3: Process Modeling**

Computer modeling permits the systematic and reliable examination of the process and further development of the product, while minimizing the expenditure of time and money for plant trials. A hot tube mill model comprised of the following modules was to be developed: piercing mill, elongating mill, cooling, induction heating, stretch reducing mill and heat treatment. A mandrel pipe mill model would also be developed. Development of such models requires thorough understanding of thermal, mechanical and metallurgical phenomena which occur in each step. A graphic user-friendly interface was to be developed. The integrated model was to be linked with materials databases and models established for selected steel grades. Model predictions were to be applied to the on-line and off-line system control.

#### **Subtask 2.4: Process Simulation**

Experiments using a laboratory piercing rig and a thermo-mechanical hot torsion simulator were planned to simulate proposed CTMP processes. Results were to be compared with predictions from process modeling to verify the proposed rolling processes and accuracy of the process models.

#### **Subtask 2.5: Process Verification**

Process recipes were to be studied through process modeling, metallurgical investigation and process simulation to verify the possible applications of products.

#### **Subtask 2.6: Product Response**

Selected mechanical properties and hardness, machinability, annealability, formability, heat treat response and corrosion resistance were investigated for various product applications. The aim was to identify the target microstructures to yield those properties.

#### **Subtask 2.7: Direct Measurement**

Development efforts were conducted aimed at delivering a system to measure the austenite grain size of hot tubes. A laser-based ultrasonic system was to be used to obtain real time grain size data by analyzing ultrasonic attenuation. The target grain size measurement accuracy was to be  $\pm 10 \mu\text{m}$  for grain sizes ranging from 15 to 70  $\mu\text{m}$ , and  $\pm 20 \mu\text{m}$  for grain sizes as large as 150  $\mu\text{m}$ . A tube's grain size profile was to be displayed in the time interval between consecutive tubes passing that point on the process line. To save on development costs, the laser-based detection system and packaging developed in Timken's LUT project was to be used if at all possible.

#### **Subtask 2.8: Control**

A feedback control system was to be developed. The system was to incorporate input from the gauge described in Section 2.7, interface to the equipment and to the integrated model, as well as to the cooling and heating devices. The goal is to have the system provide feedback control to all equipment and devices, resulting in achievement of the desired microstructure with less variability throughout the product.

## Subtask 2.1: Deformation and Heat Transfer – Fundamental Study

To lead the application of CTMP into practice, appropriate heat transfer models were developed and critical components of the tube making process were investigated. The primary effort of the heat transfer model development and deformation studies was to develop a comprehensive set of tools for computing heat transfer and thermal history throughout the tube making process. In this subtask, the necessary computer programs for rapid and controlled slow cooling (CSC) were developed; and, heat transfer relations were developed and selected for every tube making process considered. The heat transfer models were enhanced with recrystallization and austenite decomposition models.

These models, incorporated into TOM, were used to develop process recipes for CTMP and were used as the basis of inner-loop control systems. Additionally, laboratory experimentation of rapid-cooling sprays, and in-plant trials of a device using the sprays were conducted. Inverse methods were developed and used to define the necessary heat transfer coefficients (HTCs) to predict accurately the thermal history of tubes subjected to accelerated cooling using high pressure water sprays. This experimental information was critical to understanding and controlling the rapid cooling devices. Including the HTCs in the thermal model allowed the design of future rapid cooling devices that would enable CTMP technology to be practiced in the tube mill. The models developed, with their underlying thermal fundamentals were also used to design control systems for accelerated cooling devices. Finally, literature and best practices were investigated to determine a broad range of concepts related to advanced cooling of tubing.

The rapid cooling and CSC models were enhanced over the life of the project. The CSC model initially was developed in a preliminary version. The model required additional features that were evaluated and developed through laboratory and mill experimentation. The enhancement of accelerated cooling included specific software development, model verification, and detailed investigation. There were a number of enhancements made for the continued support of the models. These included enhancements to improve solution methods, to facilitate operational options, and to facilitate program modification and maintenance through large scale restructuring of the computer programs. In addition, there were enhancements to expand the suite of boundary conditions. Final microstructure predictions were coupled with the cooling models to aid in predicting and controlling aim microstructures and properties (Figure 2.1-1).

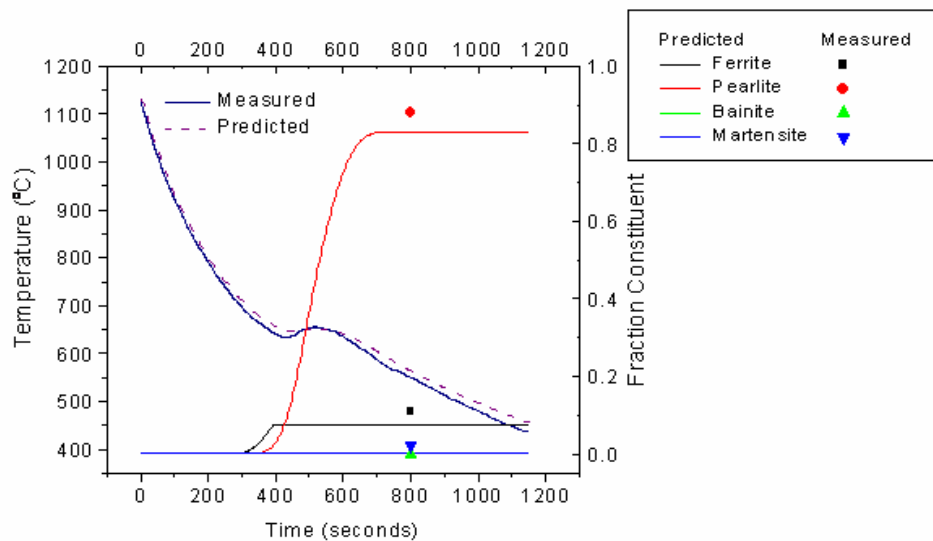


Figure 2.1-1. Comparison of CSC model to measured results.

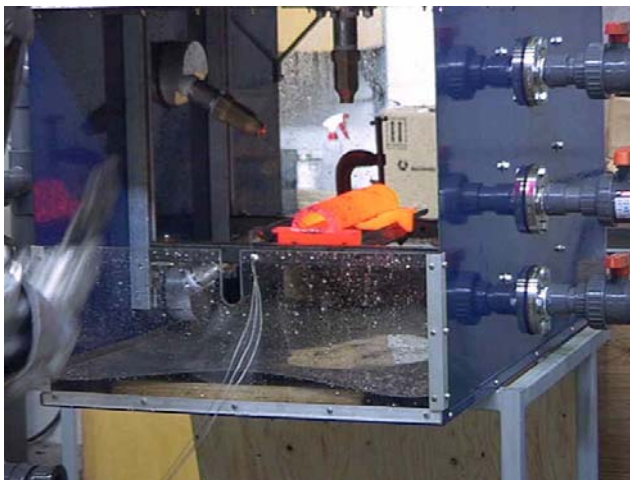
In the verification of the CSC model, a series of cooling experiments were conducted at Timken Research to acquire temperature data under various cooling conditions. The experimental thermocouple data were used to fine tune the CSC model. Then, after the addition of the austenite decomposition model, the CSC model was verified to reproduce accurately the evolution in temperatures through austenite decomposition under the conditions examined.

The capstone enhancement of the slow cool models was the further development of the model to handle stacked cooling. This additional capability enabled the optimization of the slow cooling conditions when cooling tubes in a furnace with tubes arranged in layers. Additionally, the ability of the existing equipment to meet these optimized CTMP process recipe specifications was evaluated and later validated through instrumentation of the furnace.

The inverse heat conduction (IHC) model was developed as the main tool to determine HTCs from experimental data. Originally, only a 2-D axi-symmetric version was available, but that was later modified to include microstructure evolution and a 2-D circumferential version. Once the 2-D circumferential model was completed, microstructure transformation routines for SAE 52100 steel were incorporated.

The 52100 transformation routines were necessary since the bulk of the experimental water spray testing was conducted on that steel grade. Toward the end of the project, Timken and the University of British Columbia worked together to document more fully the IHC model and adapted the program code to work interactively with a Visual Basic interface to facilitate user-friendly operation of the IHC model.

Investigations of accelerated cooling heat transfer at UBC began with literature and patent searches. Those searches laid the basis upon which initial test rig designs were developed. The experimental test rig for water and air mist sprays was constructed at UBC to study the influence of several spray parameters on heat flux. The spray rig construction utilized both, individual vertical and horizontal water sprays (Figure 2.1-2). Once the construction of the water spray test rig at was completed, the evaluation of the water spray HTCs commenced to aid in the development of specifications for the rapid cooling equipment.



(a) Hot tube segment



(b) Spray in progress

Figure 2.1-2. Rig spray test at UBC.

The spray quench rig constructed at UBC was used to conduct a four-factor DoX to determine the significant variables. Using the IHC model enhanced to fit the experimental conditions, HTC's for each test condition were determined and arranged into one algorithm to represent spray water cooling heat transfer in terms of the significant variables. Toward the end of the project, additional collaboration with UBC sought to analyze the effect of water temperature further using a water spray and air mist spray again following a DoX approach.

As in the previous thermal experiments, the tubes were instrumented with thermocouples to collect temperature-time data during spray cooling. These data were input into the IHC model to estimate the surface heat flux and related HTC's. The results were then forwarded to Timken for analysis, which was used in advanced control of quenching for CTMP recipes. At Timken with the HTC's from the UBC work, spraying equipment similar to the experimental quench rig was designed for placement after specific hot deformation processing of the tubes to enable the execution of CTMP recipes.

Concurrent with the above work, industrial designs for water spray cooling of tubes were researched through a worldwide literature and patent review on CTMP-related cooling technology conducted by Chinese Iron and Steel Research Institute, CISRI. The cooling requirements and techniques for conducting CTMP of tubes and pipes in production were evaluated. Accordingly, CISRI recommended innovative tunnel-type cooling to execute the CTMP recipes at different process stages. The initial designs were then detailed.

Toward the end of this project, it was discovered that an important aspect of conducting one of the developed processes, AFC - particularly for crack-sensitive steel grades, required oil quenching of tubes. Thus, a final activity with UBC focused on determining HTC's for oil quenching. Tests were conducted at Timken with instrumented tubes to understand more fully the oil heat transfer characteristics during boiling. The temperature data from oil quenched tubes were used by Timken to determine HTC's using the previously developed IHC model.

## Subtask 2.2: Metallurgical Characterization

### Metallurgical Models Overview

Metallurgical models were produced in support of computer-aided recipe development for CTMP, and to advance the fundamental understanding of material behavior under current and future mill processing conditions.

At conventional thermo-mechanical processing (TMP) temperatures, steel is in the single-phase austenite face-centered cubic (FCC) crystal structure. The high temperature flow stress of austenite depends on the chemistry, temperature and deformation rate. High-temperature deformation provides the stored strain energy that drives recrystallization of the austenite. After recrystallization, the austenite grains exhibit thermally activated grain growth. Upon cooling from TMP temperatures, the austenite transforms to ferrite and carbide phases, or to martensite. The final microstructure controls the mechanical properties of the as hot-rolled steel.

Models for recrystallization, grain growth, austenite decomposition and flow stress were developed for core steel grades as outlined in the project scope. These models when incorporated into computational tools aid in designing processing recipes that achieve desirable dimensional and mechanical properties in the as hot-rolled condition. For the core steels, established methods were applied in developing metallurgical models.

Beyond the core steel grades, additional testing and model development using established modeling methods were completed for selected alloys and selected processes of commercial relevance to Timken. For example, two steels which vary in composition by 0.2 wt% Mn and 0.1 wt% Ni would behave substantially the same with respect to recrystallization, grain growth, and flow stress, but would exhibit significantly different austenite decomposition behavior. In such a case, only the austenite decomposition model was developed for each steel grade, while the flow stress, recrystallization and grain growth model from the core steel grade was applied to both. The accuracy of these approximations has proved sufficient when comparing model runs to mill trial results.

In addition advanced models were pursued in the areas of austenite recrystallization and grain growth, flow stress, and data interpretation. Austenite recrystallization and grain growth was examined using a Monte Carlo Potts model, and an ISV flow stress model was used to link mechanical behavior to microstructural evolution. These models will be described further in the following sections.

### Metallurgical Model Development

#### **Grain Growth**

Grain growth was modeled using the established temperature dependent parabolic growth law model [Ref 1]. This approach has been used successfully for grain growth predictions by many investigators. Equation 1 shows the parabolic growth law model. Here  $d_0$  is the initial grain size microns,  $k$  is a constant,  $t$  is time in seconds,  $m$  is the grain growth exponent,  $Q$  is the apparent activation energy,  $R$  is the universal gas constant, and  $T$  is the absolute temperature.

$$d^m = d_0^m + kt \exp\left[\frac{-Q}{RT}\right] \quad (\text{Eq 1})$$

Steel samples were heated rapidly (30 C/sec) to temperatures ranging from 850 to 1250 C and held for times ranging from zero to 1800 seconds (Figure 2.2-1). Grain size was then evaluated using quantitative metallography. The parameters  $m$ ,  $k$ , and  $Q$  were then fit to the data to provide a grain growth model.

Grain growth models were developed for two Timken carburizing bearing grades (8119, 8219), and two carburizing automotive/gear steel grades (4027, 5130). Additional grades, found in the literature, were included in the TOM model for induction hardening medium carbon steels and high carbon through-hardened steels.

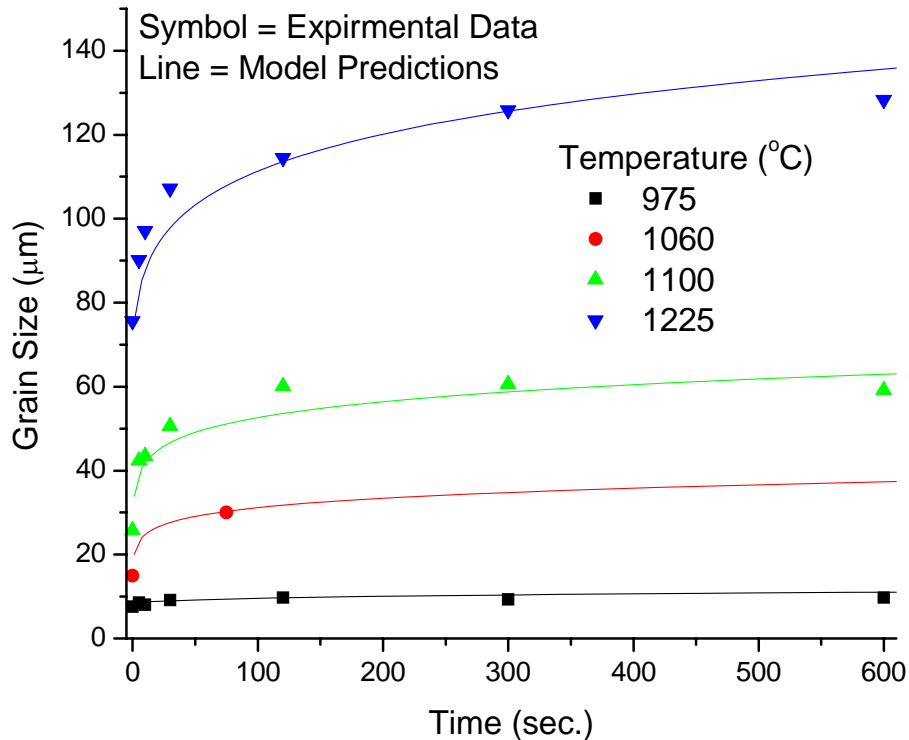


Figure 2.2-1. Modeled versus measured grain coarsening kinetics example.

## Recrystallization

Recrystallization kinetics was modeled using conventional and established phenomenological methods as well as a more advanced Potts model approach using the Monte Carlo method. Both methods will be described briefly below.

### Phenomenological Approach

The kinetics of recrystallization and recrystallized grain size were modeled using established phenomenological methods, which relate processing variables to observed recrystallization behavior [Ref 2]. This approach utilizes the well-known Johnson-Mehl-Avrami-Komolodov (JMAK) equation shown below in which  $X$  is the volume fraction recrystallized,  $t$  is the time in seconds,  $n$  is the Avrami exponent, and  $t_{0.5}$  is the time required for 50% recrystallization.

$$X = 1 - \exp \left[ -0.693 \left[ \frac{t}{t_{0.5}} \right]^n \right] \quad (\text{Eq 2})$$

For each core steel grade, a model was developed for the time for 50% recrystallization for both static recrystallization and metadynamic recrystallization as a function of deformation conditions. Static recrystallization occurs after a finite incubation period once deformation is completed. The stress strain curve under static recrystallization will not yet have reached a peak, and the material will not have begun to soften dynamically. Metadynamic recrystallization occurs after deformation that has exceeded the peak stress value, at which point the material has entered the softening, or steady state flow stress regime. Recrystallized nuclei form during the deformation event with rapid recrystallization occurring once the deformation event has been completed.

Under static recrystallization conditions, the time for 50% recrystallization is affected in the following ways: increased temperature ( $T$ ), strain rate ( $\dot{\epsilon}$ ) and strain ( $\epsilon$ ) accelerate recrystallization, while increased initial grain size ( $d_0$ ) slows recrystallization. The statically recrystallized grain size is increased with increasing starting grain size, and temperature, while increased strain and strain rates reduce statically recrystallized grain size. Equations 3 and 4 show the equations for the time for 50% static recrystallization and the statically recrystallized grain size, respectively. The terms  $A$ ,  $n$ ,  $m$ ,  $p$ ,  $B$ ,  $q$ , and  $r$  are fitting constants and the  $Q_{app}$  value is the apparent activation energy (also a fitting constant).

$$t_{0.5}^{stat} = A \cdot d_0^n \dot{\epsilon}^{-m} \epsilon^{-p} \exp \left[ \frac{Q_{app}^{stat}}{RT} \right] \quad (\text{Eq 3})$$

$$d_{srxn} = B \cdot d_0^q \epsilon^{-r} \exp \left( \frac{-Q_{app}^{srxn}}{RT} \right) \quad (\text{Eq 4})$$

Under metadynamic recrystallization conditions, the time for 50% recrystallization is also accelerated with increased temperature ( $T$ ), and strain rate ( $\dot{\epsilon}$ ). However, since recrystallized nuclei are formed during steady state flow, initial grain size and strain do not affect the rate of metadynamic recrystallization. Similarly, the metadynamically recrystallized grain size is increased with increasing temperature, and reduced with increasing strain rate ( $\dot{\epsilon}$ ), but is not affected by strain or initial grain size. Equations 5 and 6 show the equations for the time for 50% metadynamic recrystallization and the metadynamically recrystallized grain size, respectively. The terms  $C$ ,  $s$ ,  $D$ , and  $u$  are fitting constants and the  $Q_{app}$  value is the apparent activation energy (also a fitting constant),

$$t_{0.5}^{meta} = C \cdot Z^{-s} \exp \left[ \frac{Q_{app}^{meta}}{RT} \right] \quad (\text{Eq 5})$$

$$d_{mxn} = D \cdot Z^{-u} \quad (\text{Eq 6})$$

and  $Z$  is the Zener-Holloman parameter.

$$Z = \dot{\epsilon} \exp \left( \frac{Q_{app}^{def}}{RT} \right) \quad (\text{Eq 7})$$

Under TMP conditions experienced in Timken’s tube mills, steel can recrystallize in a fraction of a second. Three practical barriers exist when trying to measure the rate of recrystallization in the laboratory setting. First, it is not possible to quench a compression sample quickly enough to freeze in the state of recrystallization in all cases. As a rule of thumb, when recrystallization occurs in less than ~10 seconds one cannot freeze in the microstructure with sufficient confidence. Second, even for conditions where there is enough time to freeze in the state of recrystallization, it is often very difficult to get reliable quantitative metallography results as the austenite is not retained, and transformation products do not always decorate prior austenite grain boundaries sufficiently. And third, in cases of small strains, the size and aspect ratio of deformed grains is not sufficiently different than recrystallized grains to allow distinction in the microscope.

Therefore, double-hit compression testing was used to infer recrystallization kinetics from flow stress data [Ref 3]. In this method a sample is subject to a double-hit compression tests with a controlled inter-hit time. During the inter-hit time recrystallization processes remove the stored strain energy from the first hit. The flow stress behavior during the second compression test is affected by the amount of stored strain energy that remains. A fraction softening term is used to describe the fraction recrystallized. Here the difference between the final stress ( $\sigma_2$ ), and the yield stress ( $\sigma_1$ ) of the first compression test is used as a measure of the total strain energy imparted during the first hit. After a controlled inter-hit time, a second compression test is performed. The difference between the final stress of the first hit ( $\sigma_2$ ), and the yield stress of the second hit ( $\sigma_3$ ) is used as a measure of the softening that occurs during the inter-hit time due to recrystallization.

$$X = \frac{\sigma_2 - \sigma_3}{\sigma_2 - \sigma_1} \quad (\text{Eq 8})$$

Tests were conducted with strain rates between 1 and 100 sec<sup>-1</sup>, strains between 0.05 and 0.80, temperatures between 800 and 1250 C, and initial grain sizes between 30 and 220 microns (Figure 2.2-2). Typically a recrystallization model would be based on between 12.5-25 test conditions for static recrystallization with an additional 10-15 test conditions for dynamic recrystallization.

Recrystallization models were developed for a carburizing grade (8119), and two carburizing automotive/gear steel grades (5130, 4027). Additional grades, found in the literature, were included in the TOM model for induction hardening medium carbon steels and high carbon through hardening steels.

### **Monte Carlo Potts Model Approach**

Dr. Elizabeth A. Holm of Sandia National Laboratory and Dr. Mark T. Lusk of Colorado School of Mines were contracted as principal investigators to use advanced modeling techniques to provide more fundamental predictions of flow stress, recrystallization and grain coarsening. In the areas of recrystallization and grain growth, a Monte Carlo Potts model was employed. The key benefits of this model were that it provided a physics-based model for recrystallization and grain coarsening, which could explicitly account for particle pinning due to fine AlN precipitates at the meso-length scale.

As part of this investigation, a series of experimental steels with varied Al and N levels were melted and tested for flow stress and recrystallization via the two-hit technique. The model was successfully developed with some modifications from the original scope. These modifications were necessitated by the very fine scale of precipitates in steel relative to the conceptual work which would have required computational capabilities beyond the means of the project.

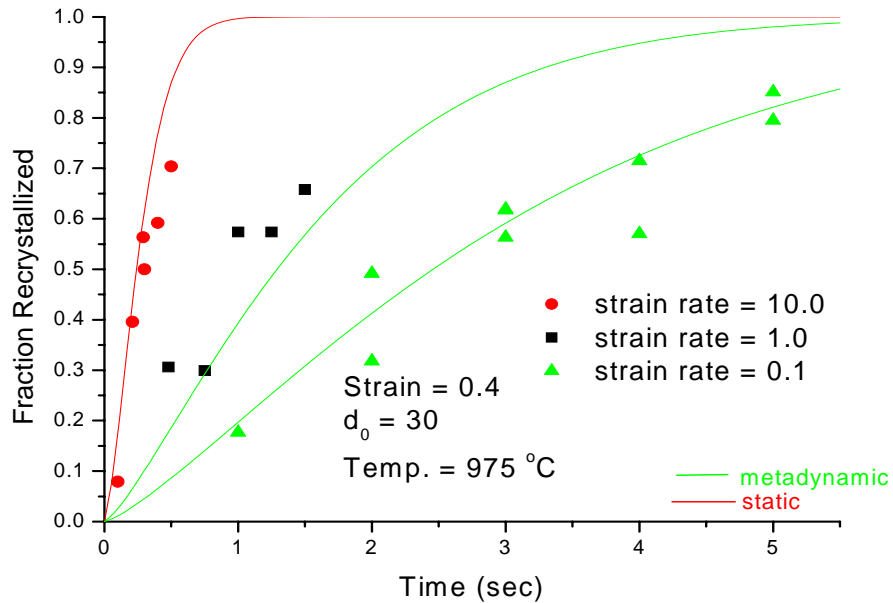


Figure 2.2-2. Modeled versus measured recrystallization kinetics example.

Paraphrasing from Miodownik, the Monte Carlo Potts model for grain growth uses a continuum microstructure which is bitmapped onto a three-dimensional (3-D) lattice by assigning each lattice site an index corresponding to the orientation of the grain in which that site is embedded [Ref 4]. Inert particles are incorporated by assigning clusters of sites a unique, non-changeable index. Sites with one or more unlike nearest neighbors are boundary sites; others are interior sites. The total energy of the system is the total boundary energy, and is computed via the Hamiltonian relation. Since the Hamiltonian does not distinguish between grain/grain and particle/matrix contributions to the system energy, the grain boundary and particle/matrix interface energies are equal in magnitude.

Grain growth is simulated by a Monte Carlo technique. First, a grain site and a neighbor orientation are chosen at random. The orientation of the chosen site is changed to the neighbor orientation with a probability. Time is incremented after each attempted reorientation by  $(1/N_g)$  Monte Carlo steps, where  $N_g$  is the number of grain (non-particle) lattice sites. Because sites may change only to a neighbor orientation, this model differs from the classical Potts model formulation. In practice, results are statistically equivalent to those generated by the classical Potts model.

For Monte Carlo Potts model, simulations of grain growth in the presence of inert, rigid, equiaxed particles, show

$$D_p = 0.728 \frac{d}{f} = \frac{2.184}{f} \text{ for } d = 3 \text{ pixels} \quad (\text{Eq 9})$$

where  $D_p$  is the pinned grain diameter,  $d$  is the particle diameter, and  $f$  is the volume fraction of particles. Grain growth in this case is strain-free and boundary properties are isotropic. The kinetics of evolution are shown in Figure 2.2-3, with  $f$  values are shown in the legend, and the particle size  $d=3$  in all cases.

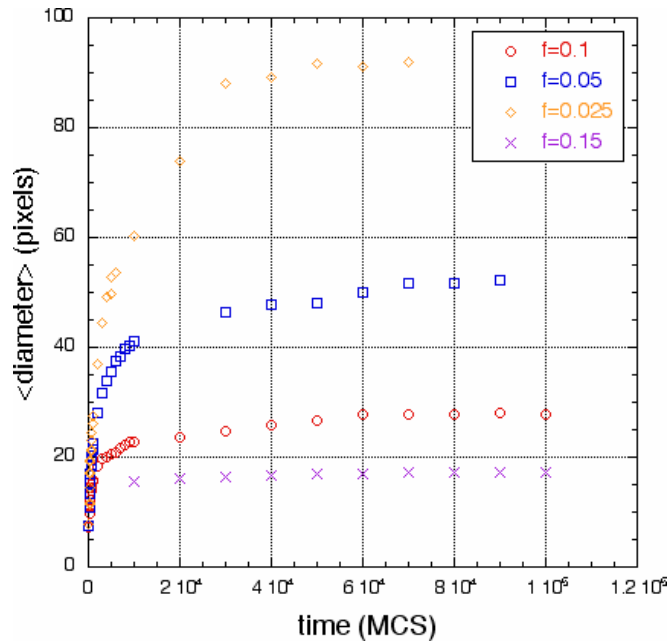


Figure 2.2-3. Monte Carlo time step versus “grain size” in the presence of Zener-pinning particles or AlN.

## Flow Stress

Flow stress models predict the stress that results when a material is subject to plastic deformation. This stress, when appropriately implemented in a computer model is used to aid in the prediction of rolling loads, plastic flow, and the evolution of product dimensional characteristics.

Flow stress was modeled using an established phenomenological approach and by using an established, but less common ISV approach. The ISV approach was pursued in order to provide a measured of stored strain energy as input in to the Potts recrystallization and grain coarsening model described in the preceding section. This will be discussed further in the section on novel methods for double hit compression data processing.

### Phenomenological Approach

An established phenomenological model was implemented to describe the flow stress behavior of core steel grades including a Timken carburizing bearing grade (8119) and two carburizing gear/automotive steels (5130, 4027). In addition models found in the literature were implemented for additional steel grades.

Flow stress was modeled in two regimes – dynamic recovery and dynamic recrystallization. In early stages of high temperature deformation dynamic recovery occurs, but much of the strain energy imparted remains causing work hardening. At later stages of deformation, dislocations begin to polygonize resulting in strain softening, and eventually a steady state stress is reached in which strain hardening and strain softening balance one another. This is referred to as dynamic recrystallization [Ref 5].

The flow stress is dependent on the strain, strain rate, temperature, and initial austenite grain size. Criteria are necessary to describe when the material is in the dynamic recovery regime, and when it is in the dynamic recrystallization regime. The model is further described in the following equations.

When strain is below a critical value, or when strain exceeds the critical value, but the Zener-Holloman value (as shown in Equation 7) exceeds the limiting Zener-Holloman value, then the materials flows stress is described by the dynamic recovery flow stress model.

Dynamic recovery when  $\varepsilon < \varepsilon_c$  or  $\varepsilon > \varepsilon_c$  but  $Z > Z_{lim}$ , then

$$\sigma^{drec} = \left[ \sigma_{ss}^{*2} + (\sigma_0^2 - \sigma_{ss}^{*2}) \cdot e^{-\Omega\varepsilon} \right]^{0.5} \quad (\text{Eq 10})$$

Where  $\sigma_{ss}^*$  is the dynamic recovery steady state stress,  $\sigma_0$  is the yield stress,  $\Omega$  is the work hardening rate term, and  $\varepsilon$  is the strain. Each of these will be described further in Equations 12-18.

When the strain is above the critical value and the Zener-Holloman value is below the limiting Zener-Holloman value, then the materials flow stress is described by the dynamic recrystallization flow stress model.

Dynamic recrystallization when  $\varepsilon > \varepsilon_c$  and  $Z < Z_{lim}$ , then

$$\sigma = \sigma^{drec} - \left[ \sigma_{ss}^* - \sigma_{ss}^{drxn} \right] \cdot \left[ 1 - \exp \left\{ -0.693 \cdot \left( \frac{\varepsilon - \varepsilon_c}{\varepsilon_{0.5} - \varepsilon_c} \right)^n \right\} \right] \quad (\text{Eq 11})$$

Where  $\sigma_{ss}^{drxn}$  is the dynamic recrystallization steady state stress,  $\varepsilon_c$  is the critical strain,  $\varepsilon_{0.5}$  is the strain for 50% softening and  $n$  is an Avrami exponent. Each of these terms will be described further in Equations 12-18. Here the terms  $A-H$  and  $a-m$  are fitting coefficients and are dependant on each steel grade. The initial grain size is  $d_0$ , and the Zener-Holloman value (Equation 7) is  $Z$ .

$$Z_{lim} = A \cdot \exp(-b \cdot d_0) \quad (\text{Eq 12})$$

$$\varepsilon_c = B \cdot d_0^c \cdot Z^e \quad (\text{Eq 13})$$

$$\sigma_0 = C \cdot d_0^{-f} \cdot Z^g \quad (\text{Eq 14})$$

$$\Omega = D \cdot d_0^h \cdot Z^{-i} \quad (\text{Eq 15})$$

$$\sigma_{ss}^* = E \cdot \left( \frac{d_0}{d_{norm}} \right)^{-j} \sinh^{-1} [F \cdot Z^k] \quad (\text{Eq 16})$$

$$\sigma_{ss}^{drxn} = G \cdot \sinh^{-1} [H \cdot Z^l] \quad (\text{Eq 17})$$

$$\varepsilon_{0.5} = H \cdot d_0^m \cdot Z^n \quad (\text{Eq 18})$$

Tests were conducted to a strain of 1.0 with strain rates between 1 and 100 sec<sup>-1</sup>, temperatures between 800 and 1250 C, and initial grain sizes between 30 and 220 microns (Figure 2.2-4). Typically a flow stress model would be based on between 22.5-40 test conditions. Flow stress models were developed for a Timken carburizing bearing grade (8119), and two carburizing automotive/gear steel grades (5130, 4027). Additional grades, found in the literature, were included in the TOM model for induction hardening medium carbon steels and high carbon through hardening steels.

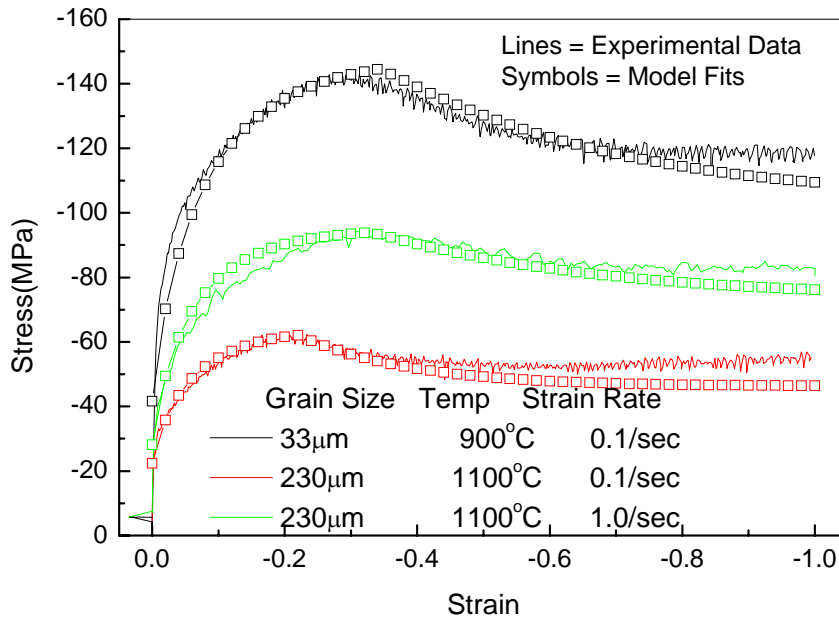


Figure 2.2-4. Modeled versus measured flow stress examples.

#### Internal State Variable (ISV) Approach

An ISV model was modified and used to simulate rate and temperature dependent deformation [Ref 6]. Because only compression tests were considered, kinematic hardening was not included. This model provided an advantage over the traditional phenomenological models described earlier in that the isotropic hardening term could both be passed to the Monte Carlo Potts model as a stored strain energy driving force, and made to evolve during the inter-hit time after the first hit. Upon the second hit, the overall flow response could then be related to both the stored strain energy and a weighted average grain size associated with partial recrystallization. This is described further below.

A novel method is used to fit both macro-scale and meso-scale models of static recrystallization using double-hit compression tests. An ISV model was adopted for the macro-scale and a Potts model was used at the meso-scale. The algorithm is applied to a class of low carbon steels. An ISV plasticity model was fitted to the first hit of double-hit compression data and used to estimate the substructure energy that drives the ensuing static recrystallization. The second-hit flow data are used to determine recrystallized volume fraction and to fit the parameters for an ISV model for static recrystallization.

This energy value was input to a Potts model of recrystallization and coarsening. This methodology was applied to a set of tests covering a range of temperatures, strains and strain rates. The ISV and Potts model predictions of volume fraction recrystallized are found to be in reasonable agreement with the phenomenological model. This method then provides a direct fit to all of the flow stress data for two-hit tests, as opposed to applying just the apparent offset yield stresses as described in Equation 8.

## Austenite Decomposition

Austenite decomposition models were pursued along two paths. A method to process and evaluate dilatometry data was developed. This data was then fit to an ISV model. This model requires rigorous investigation and data processing, but provide excellent predictive capabilities. The ISV model was developed for two Timken carburizing bearing steels (8119, 8219), two carburizing gear/automotive steels (5130, 4027), and two induction hardening grades (5046, 5150).

In addition, the MCASIS CCT and IT predictive model was re-cast in a format ready for use in FE or FD models. The QuesTek MCASIS model is less accurate than the ISV model, but has the advantage of not being grade specific. The user needs only input the steel chemistry to use the QuesTek MCASIS model in TOM.

### Internal State Variable (ISV) Approach

The ISV model uses an overall phase fraction mobility function, and a transformation rate function to predict austenite decomposition kinetics. The mobility function is considered over a normalized temperature range, and the transformation rate, which is dependant on the mobility, is normalized by the relative amount of constituent which has already formed.

Equations 19 and 20 show the mobility and transformation rate functions for the ISV model. Here  $i$  indicates the  $i^{th}$  austenite decomposition product (ferrite, pearlite, bainite or martensite),  $gf_i$  is the grain size factor,  $d_0$  is the austenite grain size,  $T_n$  is the normalized temperature and  $\Phi_{i,rel}$  is the relative fraction of constituent  $i$ . The terms  $M_{oi}$ ,  $gf_i$ ,  $a_i$ ,  $b_i$ ,  $c_i$  and  $d_i$  are fitting parameters for each constituent.

$$M_{\Phi_i} = F[d_0, T] = M_{oi} \cdot 2^{gf_i \cdot d_0} \left[ \left( \frac{T_{ni}}{a_i} \right) \left( \frac{1 - T_{ni}}{1 - a_i} \right) \left[ \frac{1}{a_i} - 1 \right] \right]^{b_i} \quad (\text{Eq 19})$$

$$\frac{d\Phi_i}{dt} = F[M_{\Phi_i}, \Phi_{i,rel}] = M_{T,d_0} \cdot \Phi_{i,rel} \left[ \left( \frac{\Phi_{i,rel}}{c_i} \right) \left( \frac{1 - \Phi_{i,rel}}{1 - c_i} \right) \left[ \frac{1}{c_i} - 1 \right] \right]^{d_i} \quad (\text{Eq 20})$$

Dilatometry tests were conducted with grain sizes ranging from 20 to 220 microns, cooling rates from -0.05 to -300 C/sec, or isothermal hold temperatures between 350 and 700 C. For each test condition the time-temperature-dilation data was converted to time-temperature-phase or constituent fraction using theoretical lattice parameter values as described further in the section entitled "Theoretical Thermal Expansion Coefficients." The ISV model was then simultaneously fit to all the data sets (typically between 30 and 50) to provide optimal values for the terms  $M_{oi}$ ,  $gf_i$ ,  $a_i$ ,  $b_i$ ,  $c_i$  and  $d_i$ .

Figure 2.2-5 shows ISV transformation model predictions for phase fraction as a function of cooling rate and prior austenite grain size for 5130 steel. This figure is representative of each of the steel grades investigated. Variations in the strength of the grain size effect were noted. Similarly, higher carbon grades (~0.5 %) exhibited significantly less ferrite, as expected, and a lesser grain size effect.

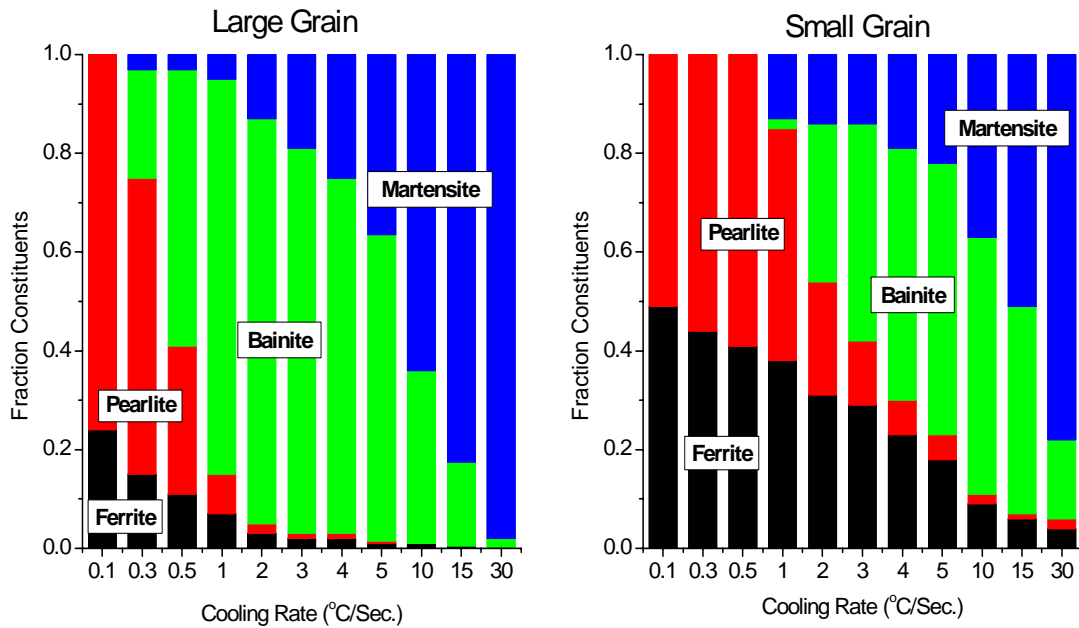


Figure 2.2-5. ISV transformation model predictions for phase fraction as a function of cooling rate and prior austenite grain size for 5130 steel.

### QuesTek MCASIS

The MCASIS program was developed to predict Jominy hardenability, as well as CCT and IT behavior [Ref 7]. Published CCT and IT curves were used to find the best fit for chemistry dependent parameters in the MCASIS transformation model. For the current project, QuesTek was commissioned to re-cast the MCASIS program into a form usable for finite difference calculation. The TOM model has the QuesTek MCASIS capability included in it and is documented in a user's and theoretical guide.

### CCT-TTT Curves

The MCASIS transformation kinetics model and implementation has been modified and improved by QuesTek through a project supported by Timken CTMP Project. The purpose of this software is to allow MCASIS model to be used within a FE or FD simulation.

The phase transformation kinetics of the decomposition of austenite during quenching are described graphically with TTT/CCT diagrams, which offer a concise illustration of transformation behavior at different temperatures and quench rates. QuesTek's implementation directly solves MCASIS state variable model. It offers a natural approach for a FE/FD simulation where the volume fraction variation is desired. The GUI front end offers a centralized and simplified operation of TTT/CCT software (Figure 2.2-6). Additionally, post-processing capability is incorporated for visualizing/comparing the TTT and CCT diagrams. With graphical components such as buttons and entry fields, it allows the user to efficiently enter and modify the necessary parameters for TTT/CCT calculation, activate calculation, and then make comparisons with TTT/CCT data from experiments or literatures.

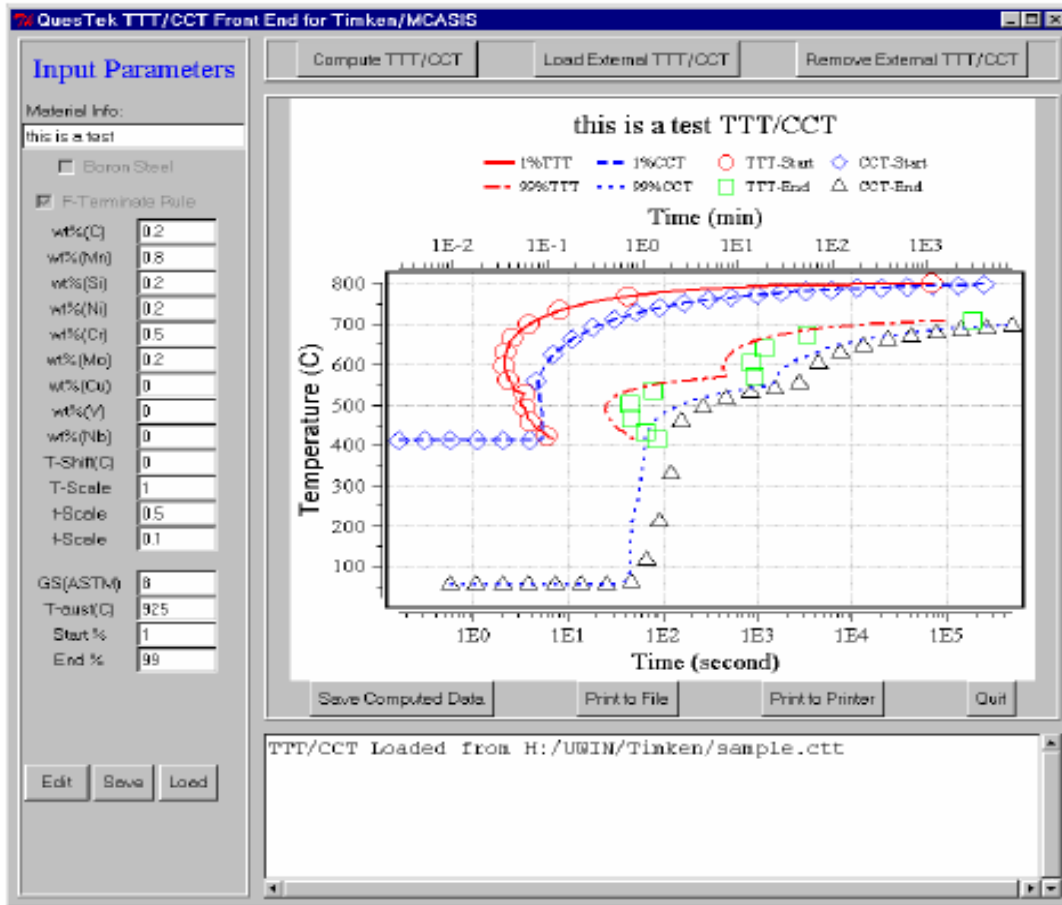


Figure 2.2-6. Interface to chemistry based CCT/TTT modeling.

### Theoretical Thermal Expansion Coefficients

Various investigators have measured the lattice parameters of austenite, ferrite, cementite and martensite as a function of carbon content and temperature. This information has proved to be valuable fundamental information which has found broad use in the CTMP project. Temperature and carbon dependent lattice parameters have been used to do the following:

- Convert dilatometry time-temperature-dilation data into time-temperature-fraction constituent data,
- Calculate theoretical thermal expansion coefficients for tubular products, and
- Predict heat treat distortion for carburized products by including theoretical transformation strain into the ISV austenite decomposition model.

The carbon and temperature dependent lattice parameters used are described below, followed by a brief description of their application to each example provided above. In Equations 21-25,  $T$  is temperature,  $X_c$  is the number of carbon atoms per 100 solute atoms,  $l$  refers to the cube lattice parameter of the austenite ( $\gamma$ ) or ferrite ( $\alpha$ ), or in the case of cementite ( $Fe_3C$ ),  $l$  refers to the cube root of the volume of the cementite unit cell [Ref 8-10]. The martensite lattice parameters ( $a_m$  and  $c_m$ ) are a function of wt% carbon. All lattice parameters are in nanometers.

$$l_\gamma = (0.363086 + 0.000752 \cdot X_c) \cdot (1 + (24.92 - 0.61 \cdot X_c) \cdot (1E - 6) \cdot (T(^{\circ}C) + 273 - 1000)) \quad (\text{Eq 21})$$

$$l_\alpha = 0.288634 \cdot [1 + (1.755E - 5) \cdot (T(^{\circ}C) + 273 - 800)] \quad (\text{Eq 22})$$

$$l_{Fe_3C} = 0.1 \cdot (153.912 + 0.008023 \cdot T_{low} (^{\circ}C))^{1/3} \quad (\text{Eq 23})$$

$$a_m = [0.28723 - 0.0013 \cdot \text{wt\%}_{carbon}] \cdot [1 + (11.5E - 6) \cdot (T(^{\circ}C) - 25)] \quad (\text{Eq 24})$$

and,

$$c_m = [0.28664 + A \cdot \text{wt\%}_{carbon}] \cdot [1 + (11.5E - 6) \cdot (T(^{\circ}C) - 25)] \quad (\text{Eq 25})$$

$$\text{wt\%}_{carbon} < 0.55; A = 0.002 \quad \text{or} \quad \text{wt\%}_{carbon} \geq 0.55; A = 0.0116$$

When the number of solute atoms per unit cell is known (Table 2.2-1), then the linear strain per solute atom can be determined as a function of temperature and carbon content for each phase. Using 100 solute atoms as a base allows for simple phase fraction calculations. In this way, the ISV transformation model coefficients can be optimized such that phase fractions predicted from the model result in a predicted dilation curve (based on phase fractions and carbon/phase dependent lattice parameters) match experimental dilation curves.

The ISV transformation model parameters were optimized to provide a best fit comparison between the measured dilation curves, and predicted dilation based on the model and theoretical lattice parameters. Quantitative metallography was used to confirm or improve the overall predictions. For a given steel grade, dilation data was collected as a function of grain size (ASTM 2-10), using both continuous cooling (0.05 to 300 C/sec) and isothermal hold (700-400 C) schedules. Typically, the ISV transformation model was fit to between 30 and 45 separate dilation data sets per steel grade. An example dilation fit and concurrent transformations are shown in Figure 2.2-7.

Table 2.2-1. Number of substitutional atoms per unit cell.

| Phase                  | Crystal Structure        | Number of subs. atoms per cell (B) |
|------------------------|--------------------------|------------------------------------|
| Austenite ( $\gamma$ ) | Face Centered Cubic      | 4                                  |
| Ferrite ( $\alpha$ )   | Body Centered Cubic      | 2                                  |
| Cementite ( $Fe_3C$ )  | Orthorhombic             | 12                                 |
| Martensite             | Body Centered Tetragonal | 2                                  |

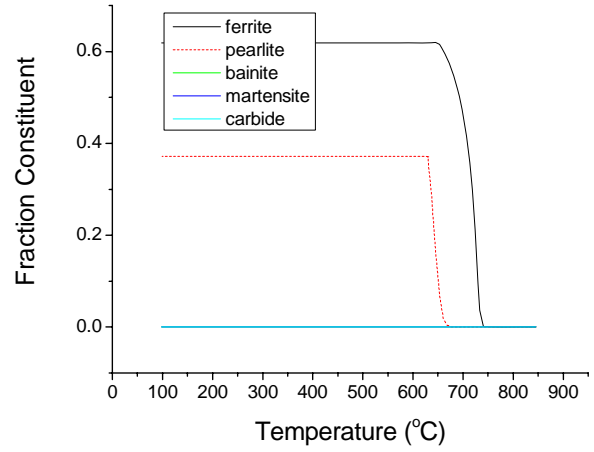
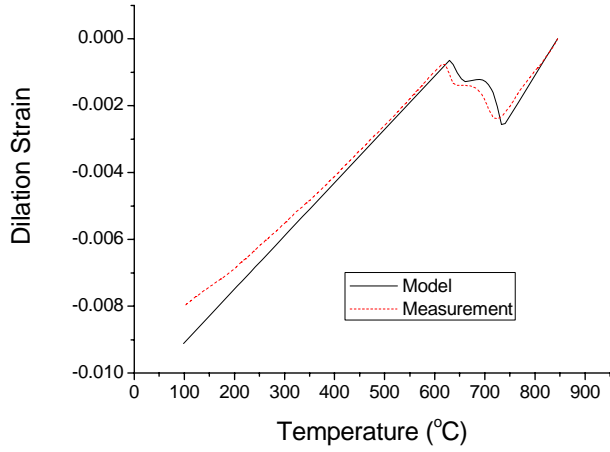
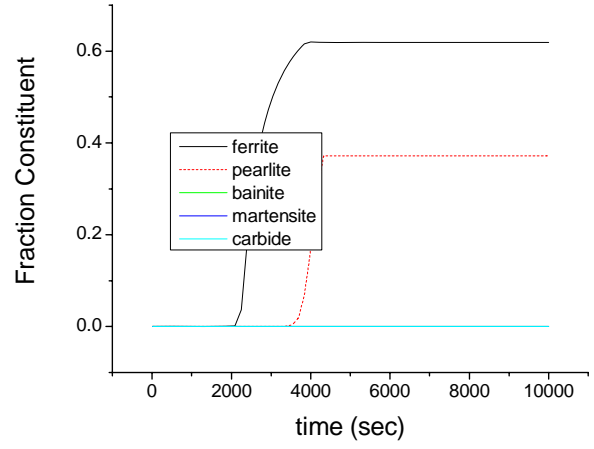
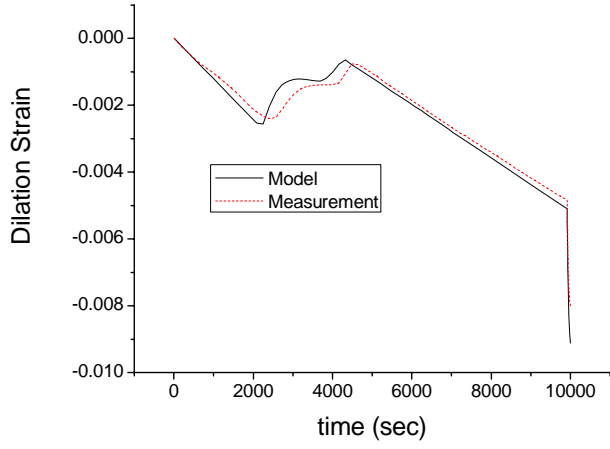


Figure 2.2-7. Example of measured and modeled dilation data and the resulting phase fractions as determined by the ISV transformation model.